Dispersal of Fry and Distribution of Redds Interact to Shape Density Dependence in Winter Steelhead of the Skagit River

Nicholas Chambers

A thesis

submitted in partial fulfillment of the

requirements for the degree of

Master of Science

University of Washington

2025

Committee:

Daniel Schindler

Mark Scheuerell

George Pess

Program Authorized to Offer Degree:

School of Aquatic and Fishery Sciences

University of Washington

Abstract

Dispersal of Fry and Distribution of Redds Interact to Shape Density Dependence in Winter Steelhead of the Skagit River

Nicholas Chambers

Chair of the Supervisory Committee:

Daniel Schindler

School of Aquatic and Fishery Sciences

The spatial scale of dispersal during early life stages when mortality rates are high is essential for understanding the relationship of the distribution of spawners to population productivity. In this study, we quantified the fine-scale distribution of age-0+ (fry) steelhead *(Oncorhynchus mykiss)* near redds across multiple sites in the Skagit River, WA. The estimated mean downstream displacement of fry was 145m with 95% of fry remained within 312m of their natal redd. Evidence of density-dependent dispersal was found at sites with multiple redds, where mean displacement increased to 270 m, though individual kernel tails could not be resolved. This limited dispersal resulted in strong spatial clustering of fry in areas with multiple redds. To evaluate effects of limited dispersal, we applied simulated dispersal kernels to ten years of spatially located redds to simulate fry distributions across a 31.5 km stream network, scaling each kernel to represent the same number of potential fry. The distance of stream channel accessed by fry increased linearly with increasing redd abundance, demonstrating spatial expansion and contraction of spawners in relation to abundance. Core spawning areas were consistently reused across years, with higher proportions in core areas in low abundance years. Increasing spawner abundance led to a shift in the proportion of fry from a majority in low density areas to a majority in high density areas. This provides strong evidence that density dependence was present across the range of observed spawner densities. Despite the change in average fry density, the number of fry in low density areas remained relatively constant due to spatial expansion of spawners. Expansion into heterogenous habitats would lead

to habitat mediated effects on recruitment, where if habitat quality is spatially uniform then expansion would increase recruitment proportionally with spawner abundance. Our findings highlight the importance of incorporating spatial structure and fry-scale dispersal into models of habitat capacity and recruitment, particularly when evaluating restoration or harvest strategies aimed at conserving the full range of life-history diversity.

Acknowledgements

This project was made possible with funding generously provided by Seattle City Light, NOAA Fisheries and the School of Aquatic and Fishery Sciences at University of Washington. Numerous individuals also provided indispensable support for the work detailed in this this manuscript. Flat out, this project would not have worked without the help of fish counters extraordinaire - Ben Culver and Kiara Milcoff. Willing to work day and night (literally), brave cold water, embrace tedious field work and most importantly maintain a great attitude: techs like this are the unsung heroes of science. Daniel always kept me honest and grounded to fundamental ecology. Mark demonstrated enduring patience with my general lack of statistical knowledge and computer skills. George was a wealth of knowledge and connections, and I admit, I am still catching up on my extended reading list. Erin Lowery at Seattle City Light was generous with knowledge and data, helping extend the scope of this work greatly. The graduate student community was tremendously supportive in assisting with fieldwork, helping with remedial mathematics and commiserating over the trials of graduate school. I could not have made it to the finish line without the tremendous support of my committee and my peers and I am eternally grateful. And last but not least, my friend John McMillan who introduced these concepts to me years ago and who, without his help, I would likely not have found this path.

Table of Contents

Introduction

Population dynamics in fishes are strongly affected by density-dependent and density-independent processes early in life, with the strongest effects typically occurring during or shortly after the larval stage (Fuiman and Werner 2002). Consequently, models of population dynamics often focus on early life stages when density-dependent mortality can strongly influence cohort strength. Compensatory density-dependent processes provide a stabilizing effect on populations where reduced offspring density at low adult abundance can lead to higher per capita growth and survival. In highly fecund species, the potential for compensation may diminish with age as life stages become less numerous and natural mortality rates decline (Wright et al. 2020). While compensatory responses are a cornerstone of models of population regulation, it remains unclear how ontogenetic changes in spatial structure influence these dynamics. In stream type salmonids for example, early life stages often experience limited dispersal and high local density in proximity to natal locations, in contrast to the broader spatial spread observed in older juvenile and adult stages (Milner et al. 2003). This shift in spatial distribution across life stages raises important questions about when and where density dependence operates most strongly. Disentangling these stage-specific patterns is essential for improving our understanding of compensatory survival and for refining our understanding of population responses to variation in spawner abundance and habitat conditions.

Spatial structure in highly migratory species is shaped by breeding site fidelity, abundance of breeders, competition among breeders, and juvenile dispersal. In both migratory birds and fishes, homing to natal sites for reproduction can increase fitness (Barbraud and Delord 2020, Peterson et al. 2014, Mobley 2019). Anadromous salmonids exhibit high breeding site fidelity to their natal streams (Quinn et al. 2006, Groot and Margolis 1991) and even reaches (Hamann and Kennedy 2012, May et al. 2023). As a result, salmonid populations exhibit strong spatial structure (McGlauflin et al 2011, Neville et al 2006), with patterns that may vary by life stage due to site fidelity and ontogenetic shifts in dispersal capacity. In spatially structured populations, adult abundance and occupancy tend to follow a positive relationship

such that more sites become occupied as abundance increases (Gaston et al. 2000). This pattern has been observed in Chinook salmon, where spawners expanded into previously unused areas as abundance increased (Isaak and Thurow 2006). This suggests the fitness benefits of homing to natal sites will be offset by increased risk of redd superimposition and high offspring density under crowded conditions. In such cases, density dependent dispersal of adults may help mitigate fitness costs and lead to broader spawning distributions (Falcy 2015, Fleming 1996). When relatively few patches are used for spawning the distribution of offspring across rearing habitat is a function of spawning location and juvenile dispersal.

Across numerous taxa, the ability of juveniles to undertake movements into new habitats varies by life stage and generally increases with body size (Roff 1991). For stream type salmonids such as Atlantic salmon *(Salmo salar)* and brown trout *(Salmo trutta)*, most fry will remain within several hundred meters of their natal redds during the first summer of life (Egglishaw and Shackley 1980, Beall et al. 1994, Foldvik 2010, Brundson 2017). Some evidence exists that steelhead *(Oncorhynchus mykiss)* fry exhibit similarly limited dispersal, although most examples rely on stocked fry (Hume and Parkinson 1987, Close and Andersen 1992, Graynoth 1999). The first summer of life is typically the period of greatest mortality after the onset of exogenous feeding (Quinn 2018). During this early period, both survival and growth rates have both been found to be density dependent for Atlantic Salmon (Gurney et al. 2008, Einum and Nislow 2005), Brown Trout (Elliott 1994), and steelhead (Wentworth and Labar 1984, Hume and Parkinson 1988, Ward and Slaney 1993, Sogard 2009). Dispersing into low-density or unoccupied habitat may lead to increased growth due to reduced competition for prey. However, dispersal is particularly risky for fry, carrying an elevated risk of mortality and uncertainty about whether suitable, low-density habitat will be found (Milner 1979).

Periods of life with limited dispersal and high mortality have important implications for population dynamics. For example, growth and mortality rates of Atlantic Salmon have been shown to be density

dependent at a spatial scale of meters to tens of meters (Einum and Nislow 2005, Einum et al. 2008a, 2011). This suggests a fitness advantage is conferred to individuals that remain close to the redd site, aligning with the expectation that dispersal is a costly strategy. If most recruitment arises from areas adjacent to redd locations, then local processes leading to variation in vital rates may explain recruitment variability better than broad scale habitat factors. Accordingly, patterns of abundance and growth established during the first summer appear to be important factors regulating cohort strength in freshwater. For example, Ward and Slaney (1993) found that the first year of life was the primary determinant of the number and size of steelhead smolts in the Keogh River, a small coastal river in British Columbia. Similarly, Crozier and Kennedy (1995) developed an index for predicting production of Atlantic Salmon smolts from age 0+ abundance for when smolt data were unavailable. This suggests the patterns set during the early fry stage can carry through to later life stages, and density dependent effects may be strongest early in life, with relatively weaker and more variable effects on parr (Vincenzi et al 2012). This is consistent with Elliott (1985) where a stock recruitment relationship explained less variation in abundance through ontogeny.

In this context, even when spawner abundance is low, localized fry densities can be higher than anticipated simply because large portions of potential habitat remain underutilized. As a result, models that ignore spatial structure may overestimate the potential for compensatory recruitment by implicitly assuming juveniles are evenly distributed across the full extent of available habitat (Finstad 2013).

Although early-life dispersal and density-dependent survival have been well studied in Atlantic Salmon and Brown Trout, relatively little is known about these processes in steelhead trout. In particular, the ability of steelhead fry to disperse from redds early in life is not well-described, and it is not well understood how the density-dependence that occurs at early life stages contributes to observed patterns of recruitment to smolt and adult stages. In this study we quantified dispersal of steelhead fry from natal redds during the first summer of life. We hypothesize that dispersal will be limited with the majority of

fry remaining within several hundred meters of their respective redds, and that dispersal of fry will generally be independent of initial density. By simulating dispersal kernels over a time series of observed redd distributions, we evaluated how density-dependent spatial clustering of redds influences the amount of habitat accessible to fry and variation in fry density.

Methods

The Skagit River is the largest tributary to Puget Sound in northwest Washington State, USA with a drainage area of 8270 km2 and average annual discharge of 473 m/s3 (Pickett 1997). The Skagit originates in British Columbia, Canada and enters the United States at river km 204 where it flows through North Cascades National Park. Much of the headwaters and major tributaries have been protected from logging and development and upslope habitat remains relatively intact. A large hydroelectric complex owned by Seattle City Light (SCL) has been in place since 1921 near at the town of Newhalem (river km 151) that marks the upper extent of anadromy. This dam complex alters the natural flow regime, artificially stabilizing flows across the year and limiting floodplain connectivity downstream.

Our study reach covered a total of approximately 44 km of the mainstem Skagit River from the mouth of the Sauk River to Newhalem. The Skagit is a large low gradient river with average wetted widths of approximately 80m in the study reach. Two distinct reaches exist in the study area, an upper reach that is relatively confined by hillslope with flows relatively strongly influenced by dam operations. The lower reach, below the confluence with the Cascade River (river km 125.5), the river is less confined with greater floodplain connectivity and the flow regime becomes more variable due to increasing influence of unregulated tributaries (Williams and Phinney 1975, Reidel et al. 2025).

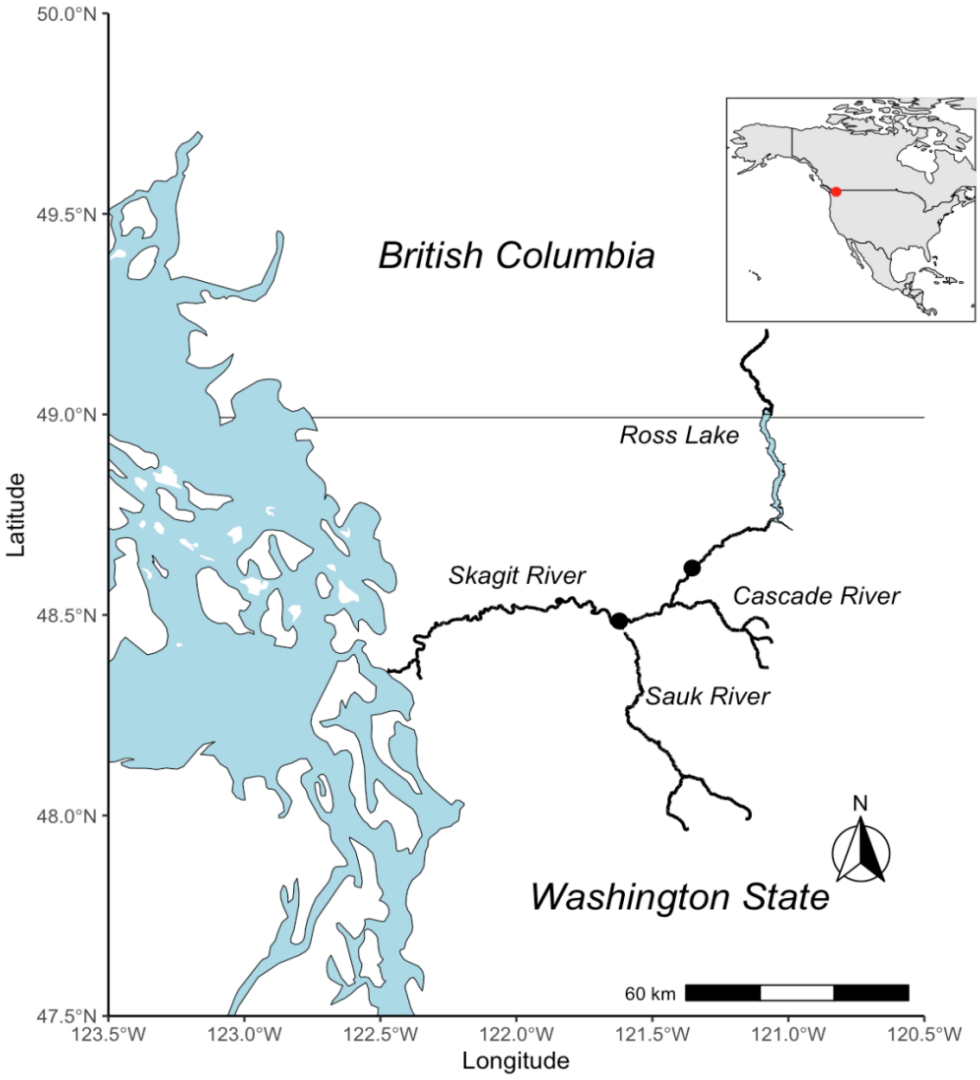

Figure 1. Data collection occurred on the mainstem Skagit River from the Mouth of the Sauk upstream to Newhalem, reach boundaries are shown by the black points on the map.

Data Collection

We used a 10-year data set of GPS located redds collected by SCL as part of a long-term monitoring program downstream of Gorge dam. Weekly redd counts are conducted by jetboat

over a 31.5km section from the Sauk River mouth (river km 107) to the base of Shovelspur rapids (river km 139). Surveys cover the period March through June, and the location of observed redds are recorded using handheld GPS. From Shovelspur upstream to Newhalem, there is less regular coverage throughout the spawning season. Beginning in March of 2022 additional weekly redd counts were conducted to extend spatial and temporal coverage of redd counts. Additional surveys were intended to increase the probability of detection of redds across the study reach in less commonly surveyed areas including the area upstream of Shovelspur and habitats, such as side channels, that were less commonly surveyed. This was intended to minimize the chance that unobserved redds would influence observations of steelhead fry.

During the summer months of 2021-2023 snorkelers documented fry distributions in relation to previously identified redds located within the 44km reach extending from Newhalem downstream to the confluence with the Sauk River. Redd locations were chosen for sampling of fry based on their fit into two categories, single or clustered. Single redds were ideally located at least 1 kilometer up or downstream from other sources of fry such as redds or tributaries. Clustered redds were defined as two or more redds within close proximity, typically within a single habitat unit, i.e. pool or riffle (Beechie et al 2005). Higher priority was given to sites with the most redds and presumably the highest densities of fry at the time of emergence. Ultimately, selection of sites was dictated by the locations fish chose to spawn and how well potential sites fit the criteria for isolation. Each site was sampled once between July and September of 2022.

Temperature was recorded on site using a handheld thermometer and from the USGS stream gauges at Marblemount and Rockport, WA. Small differences in spawn timing can have

relatively large effects on emergence timing (Austin et al. 2023), to account for this and accurately predict emergence timing estimates of emergence timing were scaled by temperature using USGS temperature gauges and an emergence timing model (Beacham and Murray 1990). Aligning sample dates across consistent times post emergence across sites to allow fry to disperse and minimize observed variation in dispersal distance due to variation in timing of sampling. Emergence of fry generally occurs over a week with a short burst of dispersal lasting 1-2 weeks after emergence (Hartman and Brown 1987, Everest 1973). Noble (1991) found that dispersal from redds was density dependent with most dispersal occurring with 14 days and declining to zero by 27 and 35 days in the two years of study. Keeley (2001) found that competitive interactions lead to size mediated dispersal patterns in artificial stream channels. Faudskar (1980) observed downstream dispersal of steelhead fry through entrainment in surface flows during crepuscular periods, and dispersal of fry was greatest among fry 37mm and under, and over 54mm. To test for similar patterns of pulsed dispersal upon emergence in the Skagit, snorkel surveys were conducted both up and downstream of known isolated redds during the first week of emergence. Locations of observed fry were marked with brightly colored markers, and distance to each marker was measured with a laser rangefinder. Dispersal distances of fry were inferred from by assuming fry were dispersing from the closest redd.

Inference of the patterns of fry dispersal from redds was made through direct observation by snorkelers working individually or in teams of two. Steelhead fry are well suited for observation by snorkelers in large mainstem rivers because they are largely diurnal (Kwain and McCauley 1978) and restricted to shallower margin habitat (Thurow 1994). Snorkeling allows long distances of streams to be covered in much less time than other methods such as electroshocking

and has minimal side effects of injury and incidental mortality (Hankin and Reeves 1988). Previously identified redds were relocated using a handheld GPS unit. Colored transect markers were laid out up and downstream of the redd at 10m intervals. At clustered sites transect layout began at the most upstream redd. Snorkeling occurred from the lowest transect and snorkelers moved upstream to minimize disturbance of fish prior to observation. When two teams were snorkeling together to cover a site, a large distance was maintained between teams each transect was only covered once. Once snorkelers stopped observing fry in at least 5 transects (50m), or snorkeling became unsafe, primarily due to current and partially submerged woody debris, then snorkeling could be stopped. As time allowed, snorkeling often continued well past the 50m point to ensure aggregations of long-distance dispersers were not missed. In areas with side channels creating islands, snorkelers covered all banks and areas that could be reached by fry without crossing the thalweg of the main channel. When fry counts became low and irregular, transects were not laid out and colored markers were placed by snorkelers to mark locations where fry were observed, and the number of fry at each location was recorded on a slate. The distance from the redd to each marker was then measured using a Nikon laser rangefinder, taking into account channel bends so that distance was measured along the bank distance, not necessarily across the shortest path distance.

Steelhead fry preferentially select shallow riffle habitats and it was sometimes not possible to count fry in water less than ~ 50mm deep, particularly if these shallow areas were greater than 1m wide and substrate was large enough to obscure free swimming fry. In these cases, visual counts were made from above water whenever possible. Juvenile Coho Salmon (Oncorhynchus kisutch) of a similar size to age 0+ steelhead were present in all sites, however in the shallow

water identification from above the water surface was typically possible by distinguishing differences in dorsal and anal fin shape and coloration.

Steelhead redds are often located on shallow cobble bars which are isolated from each other by relatively deep sections of river (Beechie et al 2005). This makes continuous snorkeling between discrete habitat units difficult. To characterize the downstream extent of fry relative to spawning locations, snorkeling was conducted in regular intervals where possible to test for long distance movement. The center point of these sampling intervals began 100m down or upstream of the last point in the continuous snorkel survey, additional points were then sampled in 100m intervals. At each point four 10m transects were snorkeled, two upstream of the midpoint and two downstream of the midpoint. GPS coordinates were taken at the midpoint of each set of additional transects. These data were used to infer the pattern of fry distribution relative to observed redd locations.

Data Analysis

Fry Dispersal:

We assumed that fry did not cross the mainstem Skagit River due to its large size and high velocity and discharge, which likely inhibit directed dispersal by newly emerged fry. While occasional long-distance dispersal may occur, we assumed such events were infrequent and contributed minimally to overall patterns of fry distribution and abundance. Because young fry are typically restricted to shallow channel margins, the stream was simplified as a one-dimensional linear network, with each bank treated as an independent observation of fry density. At one site fry were not detected for approximately 200m below a known redd. This may have reflected intra-gravel movement of fry or poor survival of the marked redd

and an unobserved redd downstream. As this pattern was only observed once, we did not adjust the model structure.

Inferring the distance moved by fry during the sampling period was accomplished by fitting parametric probability distributions to observations of fry using maximum likelihood estimation.

We tested the fit of three distributions, normal, lognormal, and gamma to observed spatial distributions of fry at single redd sites. Each distribution was fit using Markov Chain Monte Carlo (MCMC) in JAGS via the rjags package in R (R Core Team 2025). A vague prior was constructed using a truncated normal distribution based on the dispersal distance provided for Atlantic Salmon in Brundson et al (2017) and Hume and Parkinson (1987) for steelhead. The model was run for 10,000 iterations, with a burn-in of 1,000 iterations. To reduce autocorrelation, every 10th sample was retained through thinning. Convergence was assessed using trace plots and Gelman-Rubin diagnostics. Posterior predictive checks were conducted to evaluate model fit, and the best-fitting distribution was selected based on visual fit and the ability to capture the observed spread in fry locations.

To evaluate the potential for density dependent dispersal in redd clusters we expanded the single-redd model to estimate fry dispersal from clusters of redds. Where redds are close enough for dispersal kernels to overlap, individual fry cannot be unambiguously assigned to a specific redd. These models attempted to fit overlapping dispersal kernels and test for density-dependent changes in the distribution of fry.

We developed three versions of a mixture model for clustered redds, additional details are provided in Appendix 1. In the first model (Model 1)**,** each fry observation was probabilistically assigned to one of several clusters, with assignment probabilities defined by a Dirichlet distribution weighted according to the relative number of redds at each location. Fry counts at each transect were modeled using gamma, normal and lognormal distributions. Cluster locations were spaced based on observed redd offsets, with the first cluster location estimated freely and subsequent clusters positioned at known distances downstream. This model does not assume fry interact with multiple redds but rather assigns each fry to a

single dispersal kernel centered on a cluster location, enabling estimation of average kernel size and shape under varying distributional assumptions.

The second model (Model 2) was a Dirichlet mixture model where fry density at each transect was modeled as a weighted mixture of dispersal kernels from all redds in the cluster. The relative contribution of each redd was governed by a Dirichlet-distributed weight vector, allowing for partial and variable contribution from each redd to any given transect. This structure allows for substantial kernel overlap and enables inference on the relative influence of each redd on fry distribution.

In this last model (model 3), redd locations were treated as latent variables and estimated along with the dispersal kernel parameters. The number of redds per cluster was fixed, but the locations remained unknown to the model, and the observed fry locations were modeled as arising from a mixture of kernels from unknown redd locations. This model allows for full uncertainty in redd location and tests whether fry data alone can inform the spatial distribution of redds at a highly localized scale.

Reuse of Spawning Locations:

To test if redd locations were reused between years we compared the observed overlap between paired years spatial redd data to a randomly generated pattern of redds across the same linear network. For each pair of years, a fixed buffer distance was applied to each redd, and we calculated the proportion of redds from the paired year that fell within the buffer. This proportion was averaged to produce a single overlap value for each year pair. A null distribution of overlap values was generated by randomly permuting redd locations along the stream network 1,000 times. For each permutation, redd locations were assigned from by drawing from a random uniform distribution, assuming no spatial structure in redd placement. The observed overlap in redd placement between paired years was compared to the null distribution. A *p*-value was then computed as the proportion of simulated values greater than or equal to the observed

overlap. This provided a one-sided test for whether the observed degree of location reuse was higher than expected by chance. This test was repeated for all pairwise year combinations.

To quantify spatial overlap in redd locations between years, we calculated the proportion of redds that fell within a 100m buffer distance of redds from other years. For each pair of years, we computed the proportions of redds located within the buffer, these two proportions were then averaged to produce a measure of interannual overlap. The resulting values were stored in a matrix representing the proportion of shared spawning locations between all year pairs

The cluster models were run for 50,000 iterations, with a burn-in of 10,000 iterations. To reduce autocorrelation, every 10th sample was retained through thinning. Convergence was assessed using trace plots and Gelman-Rubin diagnostics. Posterior predictive checks were conducted to evaluate model fit, and the best-fitting distribution was selected based on the lowest DIC value, model diagnostics and the ability to capture the observed spread in fry locations.

Area Accessible to Fry:

To estimate how fry distribution changes with spawner abundance we calculated the length of stream channel accessible to fry using several simplifying assumptions. It was assumed that fry could not cross the mainstem Skagit River, so each bank was treated separately, then added together later to produce a single value per year. Fry dispersal was modeled as a uniform dispersal kernel with a fixed spatial extent of 312m with the upstream limit at the redd location. For each year and bank combination, dispersal kernels were placed on all observed redds, and the total accessible distance was calculated by summing the non-overlapping portions of these kernels, so that overlapping segments were counted only once. This cumulative distance represents the total area accessible to fry, based on observed patterns of redds and fixed kernel size. While this can be viewed as an index of redd clustering it is a more informative and

biologically meaningful measure for this study than traditional measures such as nearest neighbor distances. because it allows for comparisons across years to assess how the proportion the stream network is accessible to fry, and how that varies with spawner abundance and distribution.

To test whether fry habitat occupancy scaled proportionally with spawner abundance across years, we compared two estimates of potential fry density. First, we assumed each redd produced 5,500 fry and summed the annual total to estimate total fry production. We then divided this value by the maximum observed accessible area across all years, providing an estimate of expected fry density if fry had full access to the entire stream network. Second, we calculated realized fry density by dividing the same annual fry total by the accessible area in each respective year, based on observed spawner distributions. Comparing these two metrics allowed us to assess whether fry were more clustered than expected under uniform habitat use, and whether spatial expansion of spawners occurred proportionally with increasing abundance.

Simulating Fry Dispersal From Observed Redds:

We generated spatially explicit estimates of fry density in relation to observed redd locations along a linear network with a spatial resolution of 10m. Dispersal kernels were applied to observed redd locations along the stream network for 10 years of redd observations. Dispersal kernels were based on model tested fits of parametric probability distributions to observations of fry that described the mean dispersal distance and area where 95% of fry were observed. As with before, each bank was treated separately so that we were not assuming dispersal kernels could overlap when redds were at similar river km's, but on opposite banks. While some fry disperse long distance, we assumed these accounted for a small proportion of the surviving fry. Some of these fish undoubtedly contribute to overall recruitment, their numbers were assumed to be negligible.

To simply calculations, redd coordinates were reprojected onto a straight, one-dimensional network of equal length to the original (31,510m). Dispersal kernels were applied with downstream skew, simulating net downstream fry movement after emergence. Each kernel was scaled to represent the potential production of fry from a single female, using an average female fecundity estimate of 5,500 eggs for each redd (WDFW, unpublished data) and assuming 100% incubation survival. In this case ensuring consistent scaling was more important than the actual estimated fecundity. While this is unrealistic, we were not drawing inferences about the true number of fry, only relative abundance and density of fry. Thus, the number of fry in this simulation is equal to our estimate of initial egg deposition. Assuming constant egg-to-fry survival introduces some uncertainty, particularly if egg to fry survival is higher in heavily used spawning areas, this would only reinforce observed patterns of high density in clustered spawning zones. Conversely, redd superimposition in high-density areas could reduce actual fry output. However, spawner density in the study reach is in general relatively low compared to other parts of the watershed, so unaccounted for superimposition is likely minimal. That said, in systems with higher spawner density, the potential effects of redd superimposition on fry density should be carefully considered when interpreting the potential effects of density dependence across the life cycle.

Following the application of fry dispersal kernels, simulated fry densities were summarized in 10-meter bins along the stream network. For each bin, the density contribution from all nearby redds was calculated by integrating the overlapping dispersal kernels, scaled to the assumed production of fry per redd. This approach accounted for spatial overlap and the decay in fry density with distance from each redd, producing a cumulative density estimate for each 10-meter segment. The normalized area under each kernel ensured that total fry output per redd was preserved, and density was expressed relative to the contribution of all overlapping kernels within each bin. Density in this case is comparable between spatially referenced bins but is not reflective of the true amount of underlying habitat at that location on the stream. While the quantity of habitat varies across the river, it was not possible to quantify these for the extent of the study area. Because we are focusing on fry during the first 1-2 months of life this

assumption is expected to be less problematic than it might be for later life stages. Age 0+ steelhead show a preference for shallow channel margins and move to deeper water habitats once sufficient growth is achieved where their swimming performance increases (Everest and Chapman 1972). While underlying habitat characteristics undoubtably lead to differences in total habitat area between locations, even relatively low changes in density can have effects on growth and survival (Einum et al. 2008a). Thus, our density estimates provide meaningful relative comparisons across space, despite not incorporating fine scale habitat heterogeneity.

Comparing estimated raw fry density across years was hindered by a few extreme values dominating visual scale and obscuring patterns. To improve comparison of spatial distribution patterns between years, a cumulative distribution-based index was used to rank bins by their contribution to total fry count (Lawson 2006). All bins across years were sorted in descending order by fry density, and a cumulative sum was calculated and divided by the overall fry production. This yielded a normalized index value between 0 and 1 for each bin that was calculated across all years. These values were then divided into quartiles, allowing visualization of how fry were distributed across low- and high-density areas over time. To characterize spatial variation, quartiles of fry density were computed across the full range of values from all years. For each quartile, the total number of fry and number of contributing bins were summarized across years and banks.

Stock Recruit Model and Response Surface:

To simulate the effect of ontogenetic variation in density dependence in freshwater a two-stage Beverton-Holt model (Moussalli and Hilborn1986) simulating adult to smolt recruitment was simulated. This parameterization of the Beverton-Holt model contains a stage specific capacity parameter that lends itself to simulating how the ability to access the full suite of suitable habitats can shift by life stage. In our model the first stage represented the first year in freshwater. The second stage then represented the

remainder of freshwater residence. These stages are intended to represent areas where the primary growing season occurs in summer and minimal growth occurs during the winter period, where mortality may be size selective. For southerly latitudes or areas that follow different patterns the timing of stage specific transitions may be different, for instance summer can represent the survival bottleneck in Southerly latitudes while cool and wet periods from fall through spring encompass the primary growing season. In this case the first stage may more accurately represent the period from emergence through a summer survival bottleneck.

The model was specified using the form:

$$R_n = \frac{p_1 p_2}{1 + \left(\frac{p_1}{c_1} + \frac{p_1 p_2}{c_2}\right) S}$$

Where R_n is the number of recruits, p_1 and p_2 represent stage specific productivity, S = number of spawners, c_1 and c_2 represent stage specific capacity. To scale the capacity parameter at the fry stage to reflect the portion of the watershed accessible to fry, it was assumed the largest escapement was equal to the asymptotic capacity of fry.

$$c_1 = c_1 \cdot d$$

The parameter d was assigned a range of values from 0.01 to 1 to simulate how the relationship would change with the clustering of redds and resulting density of fry. This assumes more clustered distributions of redds will reduce the portion of the watershed accessible to fry thus increasing density beyond what would be expected with would be more densely packed, increasing the density dependent mortality rate. A value of d of 0.01 would indicate that fry were allowed to access only 1% of the suitable habitat area, whereas a value of 1 indicates full access to the suite of suitable habitats. When $d = 1$ the model reduces to the original form.

The 1+ to smolt stage was modeled assuming fish had equal access to all habitats by setting the c_2 capacity parameter to a value larger than c_1, thus minimizing density dependent effects beyond the first year. This assumption was made for several reasons. Primarily, our modeling approach simplified the effects of density during later juvenile residence because the goal was to simulate the effects of early life density on recruitment dynamics. The simple assumption that density dependent growth and dispersal of older parr will have no effect on smolt production is likely not valid (Vincenzi 2012), however it appears the trajectories set during the first year largely carry through to the smolt stage.

In essence, this modeling framework functions as a sensitivity analysis for the implicit assumption that the spatial distribution of fry has little effect on overall density-dependent dynamics. If this assumption holds, then varying the distribution parameter d should have minimal influence on the resulting relationship, and the output should closely resemble the model when $d=1$, indicating uniform access to all available habitats. Deviation from this expectation suggests that the spatial arrangement of redds, and by extension fry, plays a meaningful role in shaping density dependent processes during early life stages.

Results

During the 2022 field season an unusually cold and late spring resulted in a late snowmelt runoff period. Peak flows occurred on June 30th at 509.7 m^3/s at Marblemount and remained near or above 254.8 m^3/s through mid-July. Predictions for timing of emergence based on a model (Beacham and Murray 1990) estimated emergence during June for many redds created in April and May. Steelhead fry were non-detectable during day and night snorkel observations at all sites from June 20th until July 19th. The onset of emergence was highly synchronous throughout the study area where early spawned fish appeared to delay emergence until conditions were suitable. This contrasted with coho salmon fry which were numerous and ubiquitous at all sample sites during from the beginning of the survey window in June. During the first week of emergence maximum observed dispersal ranged from 47-280m suggesting that

fry movement from redds occurs rapidly after emergence, similar to prior studies on steelhead (Noble 1991, Faudskar 1980) and Atlantic Salmon (Beall et al 1994). It did not appear that steelhead fry used the high flow period to distribute themselves, rather they remained in the gravel and emerged on the descending limb of the hydrograph once they found conditions suitable. Juveniles from early spawning females apparently remained in the gravel for as much as three weeks beyond what the emergence timing model suggested. It is unclear if they were able to feed while in the gravel, or if their metabolic rate was slowed due to below normal temperatures. Interestingly, Lawrence (1941) found that 98% of rainbow trout fry survived starvation for 32 days at ~8°C, after which the experiment was stopped. This suggests they may have some flexibility in the timing of the onset of exogeneous feeding allowing for flexibility in emergence timing to match favorable conditions. However, there are likely costs associated with poor conditions during emergence such as has been found for brown trout where high flows during the emergence window significantly reduced fry survival (Cattaneo et al. 2002). These could come from displacement and starvation (Cattaneo et al. 2002) or from poor growth performance leading to delayed fitness costs (Mangel and Munch 2005).

Fry Dispersal Kernels

Fry distributions at single isolated redds were highly concentrated near known redds, producing clearly inferred patterns of localized dispersal (Fig. 6). At clustered redd sites, snorkel observations showed fry dispersing throughout the habitat unit containing the redds but only rarely beyond it. While a small number of fry were observed more than 1 km from the nearest documented redd, these long-distance dispersers were rare and were often observed in small groups of 2–5 fish. In most cases, the origin of these fry could not be confidently identified due to the absence of nearby redds. Notably, dispersal was predominantly downstream, consistent with expectations for newly emerged fry. An exception occurred at the highest-density site, where a portion of fry were observed moving upstream (Fig. 7). This likely reflected habitat structure: a long, low-gradient cobble bar provided a corridor for upstream movement,

while the downstream reach consisted of deep, swift water with limited refuge and increased predation risk.

At single-redd sites, gamma and lognormal distributions produced similar fits to the observed data (ΔDIC = 1), and both outperformed the normal distribution (ΔDIC = 35 and 34, respectively). Although the statistical fit was comparable between gamma and lognormal distributions, the gamma distribution was more flexible for implementation on the linear stream network and produced a better visual fit in posterior predictive checks. Based on these advantages, we selected the gamma distribution to describe fry dispersal kernels at single-redd sites. The mean dispersal distance was 145 meters (range: 89–319 m), and the 95% dispersal kernel width, representing the distance within which 95% of fry were estimated to occur, was 312.3 meters (range: 192.4–688.2 m) (Table 2).

Mean dispersal distance was greater at sites with multiple redds than at those with single redds, with an average distance of 270.4m, (range 89.8, 425.5), providing some support for density-dependent movement among fry. However, the estimated width of dispersal kernels, where 95% of fry were estimated to remain, were much greater with an average of 1033m (range 342.4, 1639.1m). This appeared to reflect model uncertainty in distinguishing overlapping tails rather than actual increases in fry dispersal, as these distances were generally at least as large as the observed pattern of redds at each site. The models did not reliably separate the outer ranges of individual kernel distributions at clustered sites, but they did appear to recover the central tendency of dispersal distances reasonably well. The best fitting model was Model 1, in which fry were categorically assigned to a single redd within a site. This model outperformed Model 2 (average Δ DIC of 5.3) which probabilistically assigned fry across multiple redds.

Across both Model 1 and Model 2, the Gamma distribution consistently outperformed either lognormal (Δ DIC 20.2, 30.1) and normal (Δ DIC 92.4, 90.7), respectively. DIC values were calculated per site and

averaged across sites for comparison of distributional fits within each model. Because each model estimated a unique kernel per redd, we averaged the distribution parameters for each site, and then across all sites within a model (Table 2).

The model with the lowest DIC values was Model 3 where redd locations were estimated freely. However, Model 3 was excluded from further analysis due to poor convergence diagnostics. Despite multiple chains and many iterations, this model consistently showed extreme autocorrelation, low effective sample sizes (ESS < 100), and unacceptably high Gelman-Rubin statistics ($\hat{R} > 10$ for several parameters). While the model structure may be salvageable with stronger priors, simplified assumptions, or increased iterations, it was not suitable for inference in its current form.

Abundance-Occupancy Relationship of Spawners

Redds were distributed non-randomly across the stream network and were spatially and temporally aggregated, particularly in years with low spawner abundance. In years with the lowest escapements, spawning locations were clustered within core areas (Fig. 3), and spawning expanded into less commonly used sites with increasing abundance. Redd locations showed significant spatial overlap between all but two paired years, with a high proportion of sites reused (Fig. 4, panel A). Overlap in redd site choice declined with increasing time between years, suggesting temporal autocorrelation in site use. In all but two paired years, the proportion of shared spawning locations exceeded the null expectation (Fig. 4, panel B), indicating that aggregation was temporally consistent across years.

Fry Density and Distribution

The density of fry did not respond evenly to changes in adult abundance across the range of occupied habitat. Instead, fry remained aggregated at low escapements because spawning became increasingly concentrated in core areas (Fig. 8). Density of fry increased sharply in highly reused sites while spatial

expansion led to moderate increases in low density regions, and among less commonly reused sites. As adult escapement increased, spawners occupied new habitats, increasing the area accessible to fry (Fig. 2, panel A).

During years with low escapements average fry density remained higher than if fry had maintained equal access to all habitat. During years with relatively few redds average fry density was 60–80% higher than would be expected if the same number of eggs were distributed uniformly across the maximum observed accessible area. For example, in 2023, the estimated fry density was 79.2 fry/m compared to an uniform density of 37.6 fry/m. Across all low-abundance years (e.g., <120 redds), realized densities ranged from 54 to 79 fry/m, while uniform densities would have been 30 to 38 fry/m, reflecting the influence of clustering of spawners on the density and distribution of fry (Fig. 2, Panel B).

While average fry density increased with increasing redd counts, the strength of the relationship varied across fry density quartiles (Fig 3). In low density regions the relationship with redd abundance was weakly positive, while in higher density regions the relationship was strongly positive. In years with fewer than 100 redds the highest density quartile was estimated to encompass only 3.3-8.9% of the total potential fry abundance. This is in comparison to the lowest quartile which accounted for 31.5% to 42.2% of the total fry production during those years. At the highest observed redd counts, roughly 2.5 to 3 times as numerous, the relationship was reversed. At the highest escapements, 31.3-36.1% of the potential fry production was in the upper quartile, while only 15% to 20.2% were in the lower quartile.

This supports the expectation that average fry density increases with increasing adult abundance. However, the high-density areas represent a small portion of the stream network while accounting for roughly a third of the potential fry production. This indicates strong local aggregation persists in years with high adult abundance even though spawners spread out into new habitat. In contrast, the lowest half

of the bins showed relatively little change in the number of fry with increasing redd count. When considered alongside the observed relationship where the area accessible to fry increases with redd count, this suggests two things are occurring. Spawners strongly aggregate in preferred sites but also expand their distribution into previously unoccupied sites as abundance increases.

Simulating Effects of Spawner Aggregation

The response surface (Fig. 5) illustrates how recruitment may vary as a function of both spawner abundance and spatial distribution. The upper asymptote represents a null model where fry have equal access to all potentially productive habitats. As distribution becomes more constrained, either due to low spawner abundance or tightly clustered spawning, fry to parr recruitment declines below this null expectation, even if total spawner numbers remain constant. This conceptually illustrates how spatial structure mediates density dependent compensation.

Discussion

Spatial data on the distribution of spawning steelhead is rare, and while knowledge about spatial structure has been called out as a data gap (ISAB 2015, Walters et al. 2013), few studies have been able to produce inferences regarding the effect of spatial structure on density dependence in juvenile steelhead. Our observations of the spatial distribution of fry adjacent to redds allowed us to make fine scale predictions about changes in fry density using a time series of spatially located redds across a range of adult spawner abundance. Our results align with studies on salmonids with high mortality and restricted dispersal at early life stages such as Atlantic Salmon.

A recent model for the Skagit estimated carrying capacity to be 7,700 winter steelhead spawners with a 95% credible interval of 5,900 – 12,800 (Scheuerell et al. 2020). During the years included in this study,

Skagit escapement estimates ranged from 2,502 - 9,084 spawners. This provided an opportunity to observe how spawner distributions expanded with increasing abundance, from well below estimated capacity to above. Our study reach accounted for less than 10% of the estimated winter steelhead redds in the entire Skagit, however the trends in abundance are generally correlated with overall returns the Skagit in most years. We found that spawners expanded into previously unoccupied habitats at higher escapements, while density increased in commonly reused areas. Significant spatial overlap in spawning sites existed across years where the most frequently used sites hosted a larger proportion of redds in low abundance years. This suggests that during low abundance years, spawners retreat into consistently used core areas that may represent the most productive habitats, similar to what has been observed in Spring Chinook (Thurow 2020) and Atlantic Salmon (Finstad et al. 2013).

Distributions of fry were inferred from patterns of redds, limiting our ability to explicitly test for the presence of density dependence. However, fry distributions were strongly constrained to areas near redds early in life with an average dispersal distance of 145m and 95% of fry were estimated to stay within a 312m dispersal kernel during the first 1-2 months of life. While there was some evidence of greater fry dispersal when redds were clustered, we did not observe a substantial increase in distribution that would suggest steelhead fry are able to evenly access the same spatial extent of habitats when spawner distributions were patchy. Even when multiple dispersal kernels overlapped, we did not observe an increase in long distance dispersal leading to occupancy of new habitat units.

We found that average fry density increased with spawner abundance, but the increase was not evenly distributed across the habitat mosaic. Rather, our results suggest redd and fry density increased sharply in the most highly reused core areas. Despite a marked increase in fry abundance, the highest density quartile accounted for a small portion of the total stream channel, where the highest density regions of the stream network were predicted to occupy only 60-1,310m of habitat, accounting for only 0.5% – 6.8% of the total area occupied by fry. In contrast, low density areas were estimated to host a relatively consistent

number of fry across the range of spawner abundance. This gradual increase in the number of fish in low density regions was due to spatial expansion, where redds were placed in less commonly used habitats as spawner abundance increased. Similarly, the proportion of fry which occupied high- and low-density sites was not constant across escapements. Instead, the proportion of fry in high density regions increased, while the proportion in low density areas decreased. Changes in fry density resulting from variation in the distribution and abundance of spawners likely translates to density dependent growth and/or survival.

Our results demonstrated that restricted dispersal of fry and spatial aggregation of spawners limits the proportion of the watershed used by fry during the first few week's post emergence. The relationship between the area accessible to fry and the number of redds is expected to be asymptotic as spawning sites are finite, and saturation of habitat will eventually lead to increasing overlap of dispersal kernels (Finstad et al. 2013). The pattern observed with the data available for the Upper Skagit did not reveal an asymptotic relationship (Fig. 2, Panel A) but it is unclear if this is due to underutilization of habitat or insufficient data at the highest escapements. Regardless, aggregation of spawners was predicted to lead to a more than 50% change in habitat occupancy by fry across the observed range of spawners. Together, our findings suggest density dependent signals may emerge from highly localized aggregations even across relatively low return years.

The highly limited dispersal we observed suggests the fry stage may serve as an underappreciated point of population regulation for steelhead. When patchy spawner distributions impose spatial constraints on access to rearing habitat for fry, per capita survival and growth may be reduced over what would be expected from more even distributions (Einum et al. 2008). Although our study was unable to make inferences about the effects of initial fry densities on growth and survival, the spatial patterns we demonstrated are consistent with those associated with studies showing the fry stage plays an important role in regulating population dynamics of Atlantic salmon (Crozier and Kennedy 1995, Einum and Nislow 2005, Finstad et al. 2013), which show similar patterns of restricted movement and high mortality

early in life. Compensatory body growth and survival later in freshwater development could partially buffer early spatial limitations by increasing survival among parr and smolts (Einum et al. 2008b, Vincenzi et al 2012). However, body size at the end of the first summer of life is a strong predictor of smolt age (Ward and Slaney 1993) suggesting later stages may not reverse early effects on body growth. Mangel and Munch (2005) highlighted that compensatory growth may come at a cost, suggesting a fitness advantage to spending additional year(s) in freshwater vs. maximizing short term growth. Moreover, generally high mortality rates during the first year (Bley and Moring 1988) limit the potential for later life stages to compensate numerically for losses at the fry stage.

Recruitment Patterns

Accurately describing population dynamics from inferred distributions of fry density is difficult, and especially so when stream habitats are heterogenous. Our results appear to align with theoretical expectations that the highest quality sites in a reach are expected to be occupied first (Charnov 1976), and as spawner abundance increases distribution expands (Gaston 2003). For example, we found potential for density dependent growth and/or survival among fry in core sites, and evidence of broad spatial expansion of spawners with increasing abundance. Expansion of spawners into new sites can have varying effects on recruitment, which will be dependent on the underlying habitat quality. If newly occupied sites are poor quality and function as population sinks, then they will contribute minimally to overall recruitment because survival will be poor. Conversely, if the habitat is suitable then newly occupied sites can offset declining per capita survival in core areas as density increases. As a result, broad patterns of survival and growth can reflect multiple processes that are a product of aggregation of spawners and underlying quality of incubation and early rearing habitat. This is consistent with findings from Ward et al. (2007) who showed that competition for space among stream type salmonids leads to density dependent growth when high-quality sites are rare and occupied first. Their model supports the idea observed growth patterns arise not only from density, but from the distribution of site quality. Thus, knowledge about the distribution and density of fry in conjunction with underlying habitat quality would improve the reliability

of inferences about the spatial scale and location at which density dependent changes in growth and per capita survival occur.

Numerous studies have attempted to quantify age specific habitat preferences of juvenile steelhead such as habitat type (pool, riffle, etc.), gradient, velocity and cover type (e.g., Bisson et al 1988, Bjornn and Reiser 1991, Gallagher et al. 2014). While they may be locally relevant, these characteristics often contradict each other and do not consistently scale across sites (McMillan et al. 2013) or between streams (Fausch 1988, Dunham and Vinyard 1997, Gibson et al. 2008). This suggests habitat quality is complex, and juvenile steelhead are able to use a wide variety of habitats. Accordingly, juvenile steelhead are widely distributed in the Skagit River and are associated with a variety of habitat types (Beechie et al. 2005). Inconsistent patterns of occupancy with physical habitat features suggest underlying habitat quality may not be solely responsible for the productive potential of habitats. For example, Issak et al. (2007) found that for spring Chinook salmon, patch size and connectivity were stronger predictors of core spawning locations than traditional measures of habitat quality. Core spawning areas may produce more smolts than less commonly used areas, not only because of underlying quality, but because they are large and relatively well connected, making them resilient to local stochasticity. Small patches could exhibit classically productive habitat types, but weak connections to nearby habitats could increase their susceptibility to stochastic survival for immobile life stages such as fry. Peripheral habitats may thus be more prone to extinction and recolonization independent of underlying quality, consistent with meta population theory (Schtickzelle and Quinn 2005). Occupancy of individual patches across spawning stock sizes would then be a function of size, connectivity and underlying habitat quality (Fullerton et al. 2011).

Compensation

Aggregation of spawners and density dependent mortality among low mobility fry complicate interpretation of density dependent signals at later life stages, particularly in spatially structured

populations that may be near or below productive capacity their watershed. For example, density dependent survival or growth may arise among fry through localized competition, not from a system-wide limit on juvenile carrying capacity (Imre et al. 2005, Einum et al. 2008, Matte et al. 2021). While density dependent survival may be strongest in high density areas, density dependent changes in body growth are often strongest at low densities (Crisp 1993, Jenkins et al. 1999). Both survival and growth rates may be density dependent at the scale of meters to tens of meters (Einum et al. 2008a, Einum et al. 2011), although some studies (e.g., Jenkins et al. 1999) have found density dependent growth at larger spatial scales only. This suggests highly localized aggregations of spawners can create density dependent signals even if productive capacity of a watershed has not been reached.

Due to the variability in escapements over our time series of data, where several years were below the estimated productive capacity, fry to smolt recruitment would be expected to change through compensatory mechanisms. In this case, increasing recruitment with spawner abundance may have been a result of higher fry production within core spawning areas, and/or increasing utilization of the habitat mosaic. We found that at the lowest spawner abundances, fry had access to only 47% as much area as the highest, and fry density was 60-80% higher than would be expected if fry were uniformly distributed across the maximum estimated occupied area (Figure 2, Panel B). This limited spatial access could suppress the expression of compensatory increases in survival, potentially even when additional suitable habitat exists. Because fry density is determined by local densities of spawners, our results suggest compensatory survival does not occur uniformly across the habitat mosaic. Rather, it arises from localized variations in fry density across occupied habitats (Figure 3), This spatial bottleneck to compensatory potential is illustrated by the response surface (Figure 5) where the inflection point is a function of the number of spawners and the occupied extent, rather than total system capacity. Thus, the annual limit for compensatory recruitment may not set by the total carrying capacity of the system, but by the area of habitat that is occupied.

In spatially structured populations with limited juvenile dispersal additional criteria for assessing the productive capacity of the habitat may be prudent. Additional signals of habitat saturation such as an asymptote in smolt production and/or the area accessible to fry would provide stronger inference about spawner and juvenile capacity. While our results point toward gradual expansion and under compensation, other theoretical outcomes are possible. For example, strict compensation would occur where expansion of spawners into new habitats perfectly offsets decreased survival rates in clustered sites due to increasing density. Alternately, overcompensation is possible where expansion of spawners into poor quality sites leads to reduced per-capita survival across all habitats as escapements increase. Additionally, populations that exhibit high spatial and temporal synchrony may experience more intense density dependence at immobile life stages than those with asynchronous spawn times and locations.

Stock Recruit Modeling

Stock-recruitment models such as the Ricker (1954) and Beverton-Holt (1957) equations provide useful approximations of fish population dynamics, but the simplifying assumptions inherent to these models mean they should be applied cautiously to species with complex life histories. Both Ricker (1963) and Beverton and Holt (1957) emphasized that small perturbations in exploitation or structure could produce unpredictable effects on recruitment and cautioned against simple interpretations of stock-recruit relationships. In species such as steelhead with many overlapping age classes and life histories (e.g. Hodge 2014), where early spatial constraints and variations in stage-specific survival can influence recruitment (Ward and Slaney 1993), stock-recruit models may miss important aspects of recruitment dynamics. For example, in a long-term study of anadromous brown trout, Elliott (1985) found that a Ricker curve produced a remarkably good fit to early life mortality of brown trout, and the explanatory power of initial egg density on recruitment declined across life stages. This suggests strong early life density dependence, and less predictable patterns of survival through ontogeny. Although the Ricker curve fit the data closely, Elliott (1996) showed it missed some underlying dynamics. Specifically, the

same fry density could result from different egg densities, with higher egg densities producing more smolts despite strong density dependent mortality. This reflexive pattern implies that spatial expansion or density dependent dispersal may allow continued increases in total recruitment even as per capita survival declines. This dynamic would be difficult to detect with traditional methods.

Strong aggregation during periods of high natural mortality and low mobility may create a scenario where the effective watershed size changes to reflect the dispersal of spawners. In years with sparse and uneven distributions of spawners productive habitats may be left unused, while crowding within core areas may still produce a signal of a capacity ceiling. As a result, stock-recruit relationships may display asymptotic patterns, a hallmark of carrying capacity, even though a portion of the system's true habitat potential remains untapped. Similarly, the potential for compensatory recruitment is constrained because fry do not have equal access to all potentially suitable sites. Thus, apparent density dependent regulation may not strictly be a signal the population is at equilibrium with its environment, only the occupied portion.

Moving forward, management frameworks that integrate spatial distribution and stage-specific dynamics will be essential for rebuilding and sustaining steelhead populations. Restoration projects aimed at increasing habitat quantity or quality are unlikely to yield substantial increases in juvenile production if escapements remain too low to promote spatial expansion into restored habitats. Without sufficient spawners to overcome initial spatial constraints and saturate newly available areas, the benefits of restoration may not translate into observable gains in abundance. Restoration and recovery planning may need to explicitly link habitat improvements with corresponding increases in escapement targets to realize the full benefits of expanded rearing capacity.

Our findings align with other studies which indicate that spatial structure and fry dispersal limitations can generate strong density-dependent signals even when large portions of habitat remain unoccupied. This

has major implications for how we infer carrying capacity, set spawner abundance goals, and evaluate the effectiveness of habitat restoration.

Despite extensive evidence from Atlantic salmon, the potential for early-stage spatial constraints to drive freshwater production has been less widely recognized among Pacific salmonid populations. Our findings, combined with the established mechanistic understanding from Atlantic systems, strongly suggest that fry-stage processes deserve greater attention in Pacific salmonid ecology and management. Management strategies that ignore the spatial dimension of density dependence risk enshrining a shrunken distribution as the long-term limit of the population.

Permits and Ethical Approval

All research involving live steelhead fry was conducted in accordance with federal and institutional guidelines. Fieldwork and handling procedures were authorized under permits issued by the National Oceanic and Atmospheric Administration (NOAA), protected species permit number 2614, and approved by the University of Washington Institutional Animal Care and Use Committee (IACUC), protocol number 4546-01.

Tables and Figures

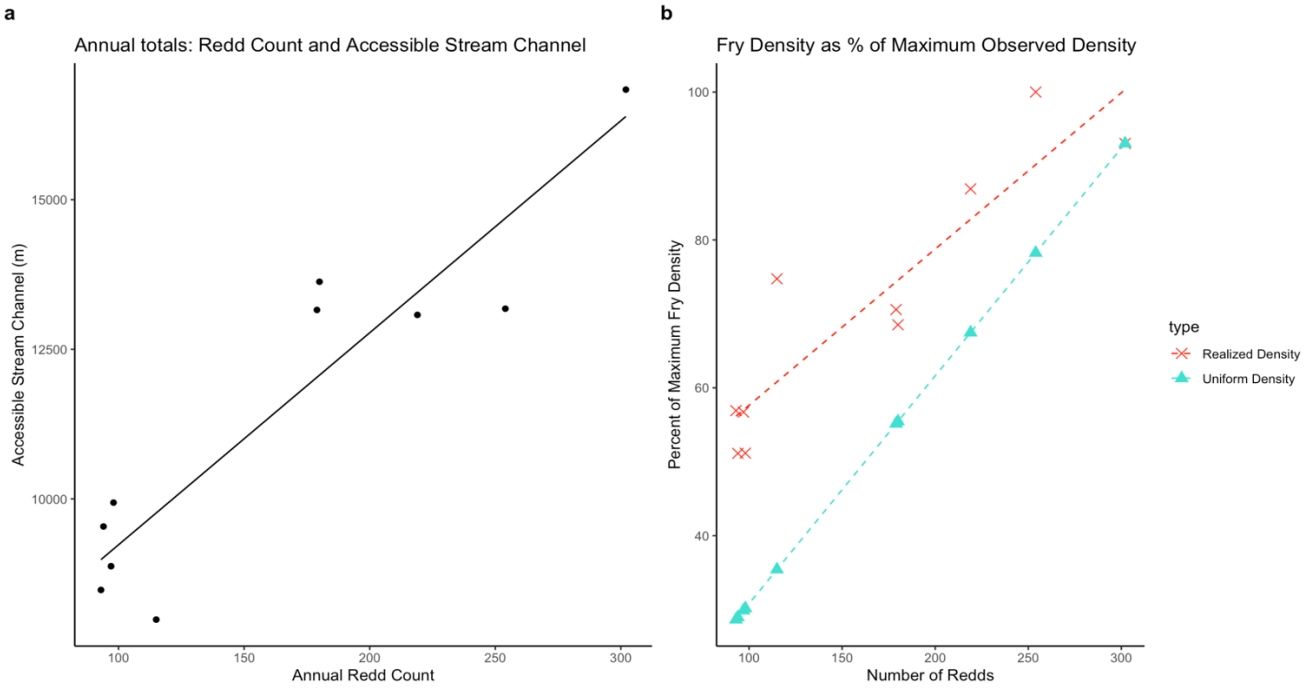

Figure 2. The area accessible to fry increased with the annual number of redds. The lowest area was 47% of the maximum observed, while the number of redds increased roughly three-fold (panel A). The realized density (red x's) is the estimated annual egg deposition divided by the accessible area for the same year. The density (blue triangles) is the annual estimated egg deposition divided by the total habitat capacity.

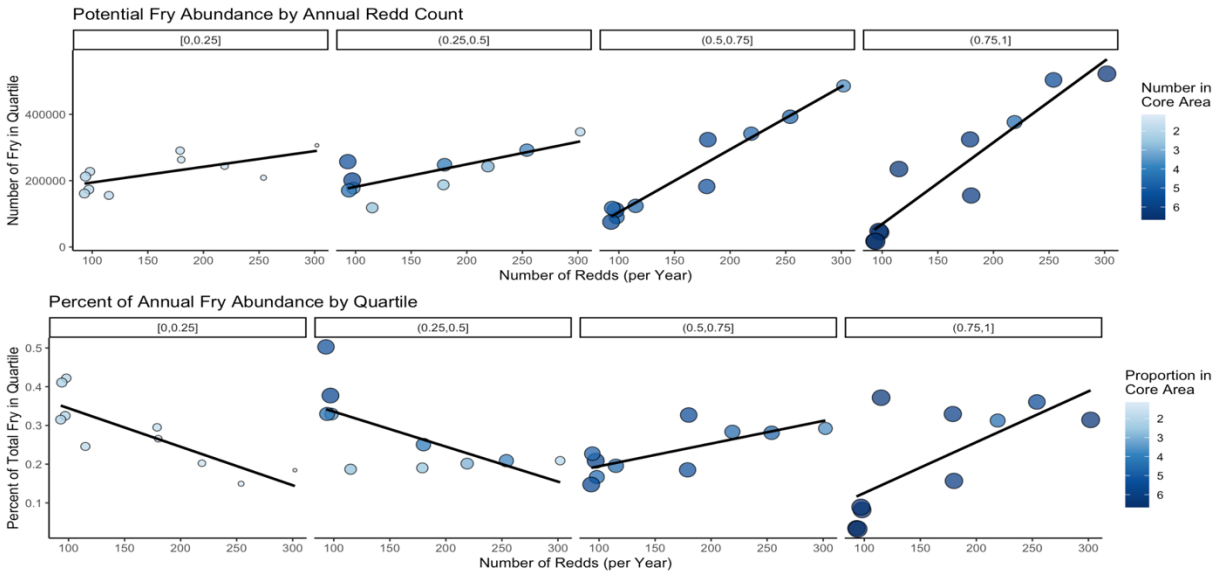

Figure 3. Each dot represents one year of data; the size of the dot and color corresponds to the proportion of spawning sites within 100m segments of channel that are re-used across years. At low spawner abundance the rate of site reuse increases suggesting that spawners retreat into core locations during poor years, and expand their distribution as abundance increases.

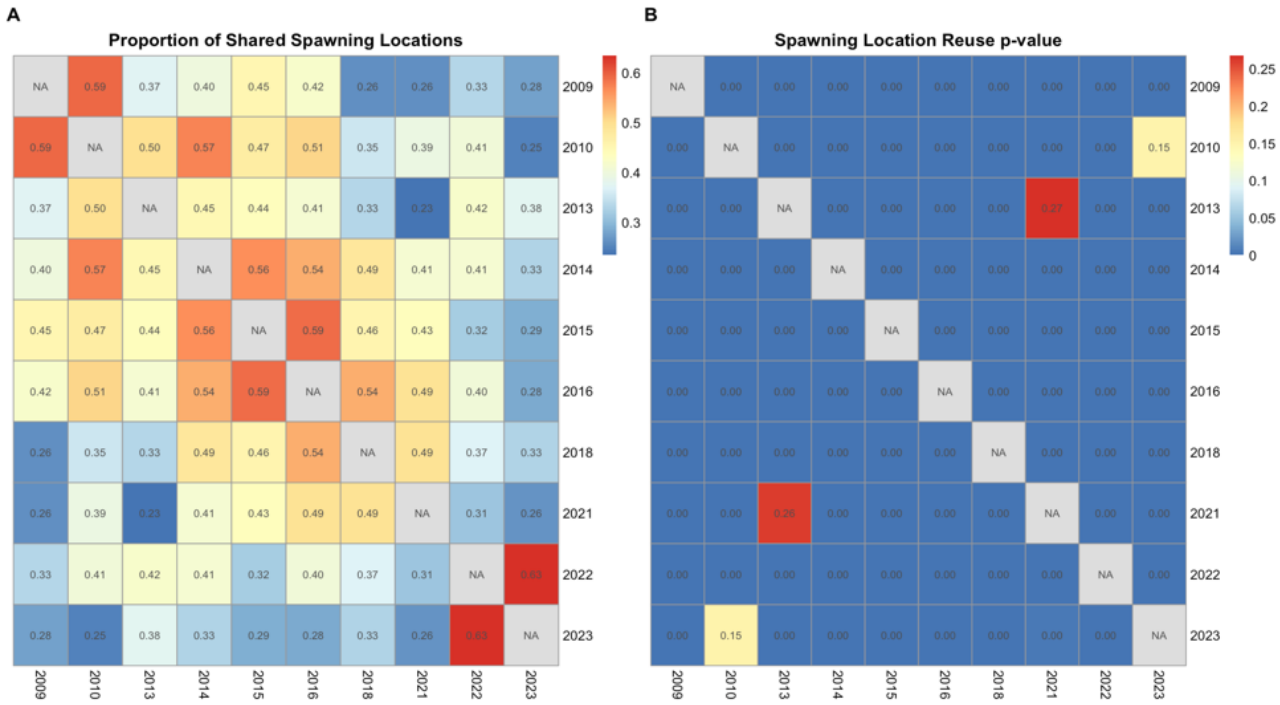

Figure 4. **A.** The proportion of redds found within a 100m buffer applied to observed redds, paired by year. the proportion of redds that shared spawning locations ranged from 23.4% to 63.4% **B.** All but two years showed significant spatial overlap in spawning areas ($p < 0.05$).

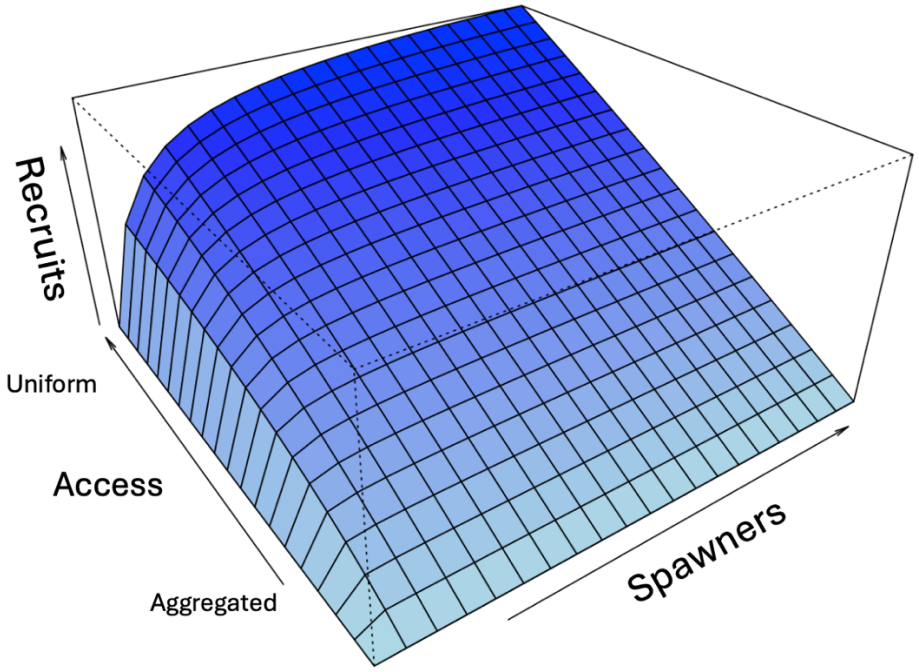

Figure 5. The response surface illustrates the conceptual interaction between spawner abundance and spatial distribution, where the two components interact to control the number of recruits. The upper most line with the highest asymptote represents the null model where the distribution of spawners equals 1 and juveniles have equal access to all habitats. When fry are spatially constrained at low spawner abundance or due to highly clustered spawning, recruitment will be limited more than the null model would predict.

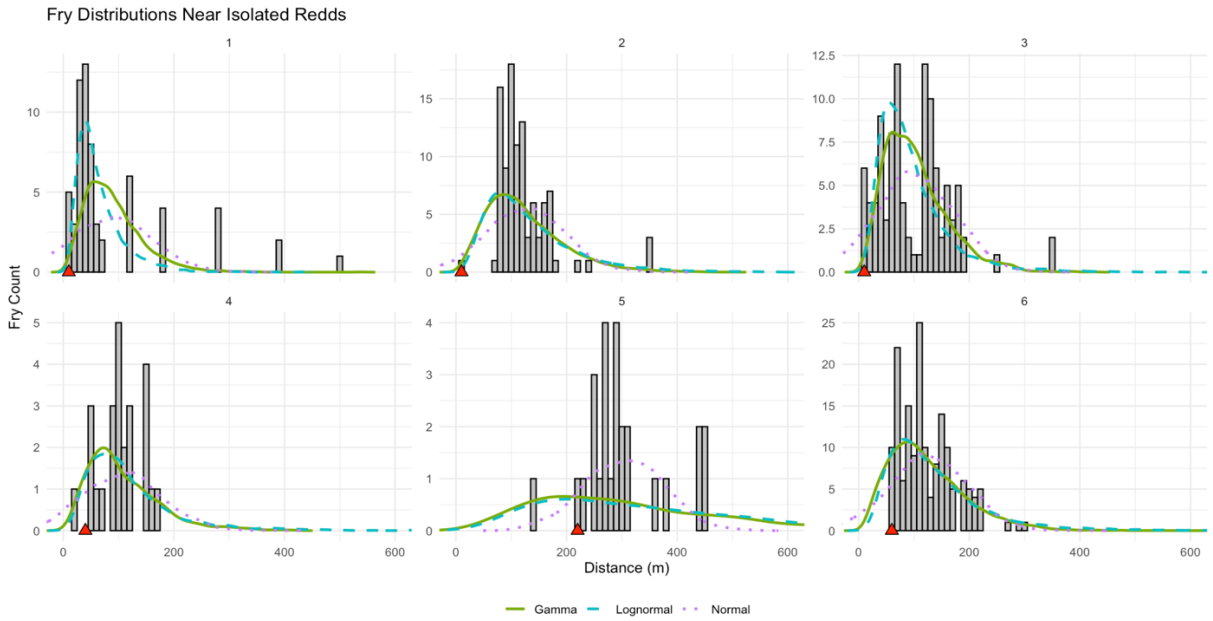

Figure 6. Observed fry are shown as counts per 10m transect, observed redds are shown by red triangles. Stream flow was from left to right at all sites. Fitted distributions are shown for each parametric probability distribution tested.

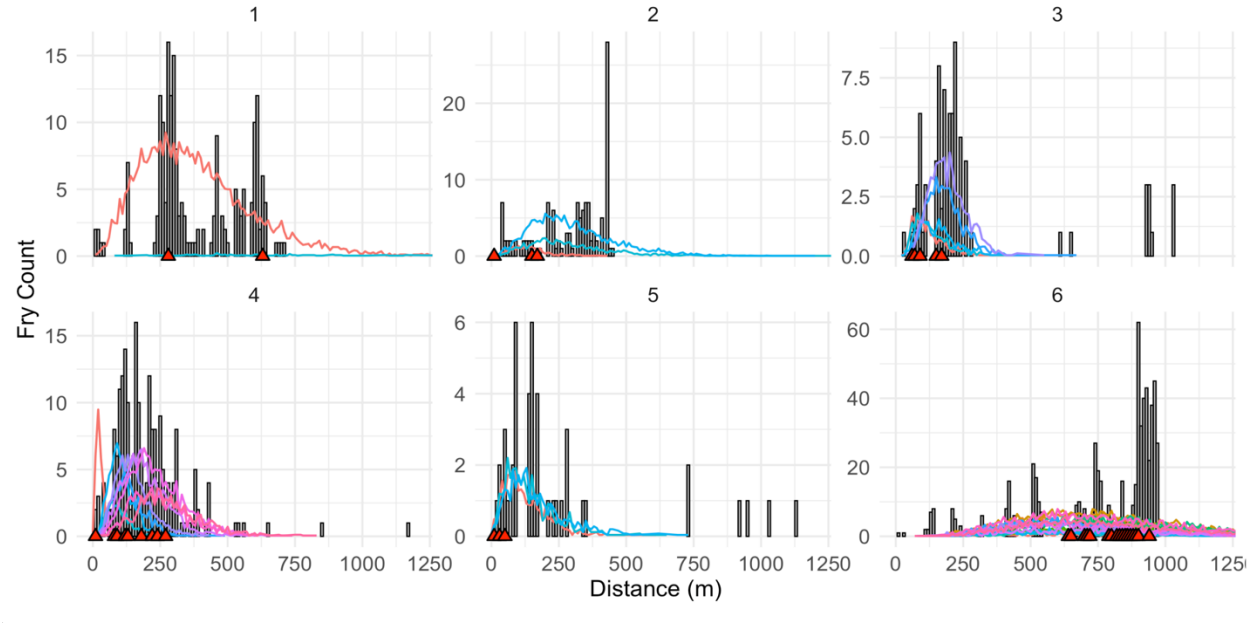

Figure 7. Observed fry are shown as counts per 10m transect, observed redds are shown by red triangles. Stream flow was from left to right at all sites. Fitted gamma distributions are shown for each redd from the best fitting model.

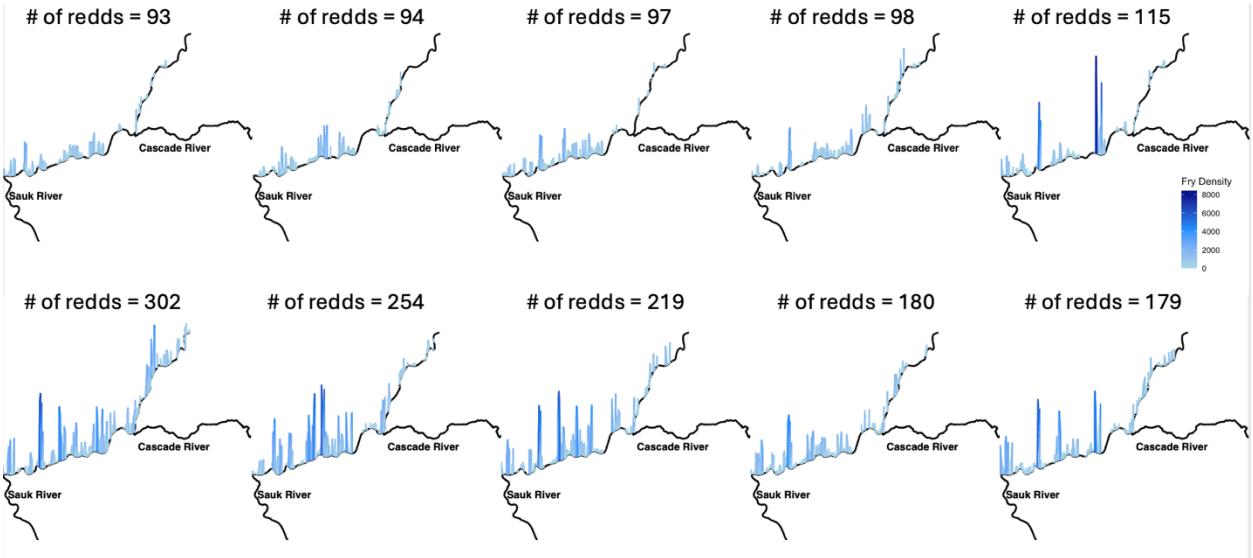

Figure 8. Simulated density of fry shown from application of gamma dispersal kernels to observed patterns of redds are along the Skagit River for the 31.5km study reach. Each panel corresponds to the number of redds observed for a given year.

	Lowest fry density (0-25%)			Moderate fry density (25-50%)			Moderate fry density (50-75%)			Highest fry density (75-100%)		
Redd Count	Number of fry	% of total fry	Occupied stream (m)	Number of fry	% of total fry	Occupied stream (m)	Number of fry	% of total fry	Occupied stream (m)	Number of fry	% of total fry	Occupied stream (m)
93	161,127	31.50%	10,170	257,165	50.28%	2,640	75,430	14.75%	440	17,786	3.48%	60
94	212,376	41.08%	12,430	170,410	32.96%	1,820	117,382	22.71%	610	16,816	3.25%	60
97	173,388	32.50%	10,030	201,221	37.72%	1,990	111,367	20.87%	590	47,522	8.91%	150
98	227,513	42.21%	12,770	177,538	32.94%	1,830	89,864	16.67%	450	44,080	8.18%	130
115	155,413	24.57%	10,450	118,219	18.69%	1,190	123,811	19.57%	670	235,057	37.16%	400
179	290,463	29.50%	16,500	187,336	19.03%	1,920	182,350	18.52%	960	324,366	32.95%	780
180	263,189	26.59%	15,780	247,981	25.05%	2,530	323,618	32.69%	1,770	155,187	15.68%	450
219	243,742	20.24%	13,830	242,660	20.15%	2,480	341,627	28.36%	1,770	376,487	31.26%	900
254	208,864	14.95%	12,990	291,961	20.90%	2,840	392,544	28.10%	2,010	503,637	36.05%	1,310
302	306,343	18.44%	17,520	347,100	20.90%	3,560	485,367	29.22%	2,410	522,193	31.44%	1,310

Table 1. The length of stream channel occupied by large numbers of fry is relatively small in years with high redd counts. In the two years with the highest redd counts, 64.2% and 60.6% of the fry were in 3.32 km and 3.72 km of the habitat, or approximately 5.5% of the total stream channel. Conversely, in the lowest density years 74.1% and 81.8% of fry were in the lowest two quartiles and covered 14.25 km and 12.81 km of stream channel, respectively, roughly 20-23% of the total stream channel.

Model	Distribution	Mean Distance	95% Kernel Width	DIC	∆ DIC
Single (model 1)	Gamma	145	312.3	5653	0
Single (model 1)	Lognormal	134	390.9	5654	1
Single (model 1)	Normal	141.74	278.3	5788	135
Cluster (model 2)	Gamma	270.4	1032.9	3051.3	0
Cluster (model 3)	Gamma	193.2	744.1	3056.6	5.3

Table 2. Mean dispersal distance is the mean of the dispersal kernel and represents the dispersal distance of the average fry. The 95% dispersal kernel width is the distance of the stream channel where 95% of fry are expected to occur.

Literature Cited

Austin, C. S., Torgersen, C. E., & Quinn, T. P. (2023). Who spawns where? Temperature, elevation, and discharge differentially affect the distribution of breeding by six Pacific salmonids within a large river basin. *Canadian Journal of Fisheries and Aquatic Sciences*, *80*(8), 1365–1384. https://doi.org/10.1139/cjfas-2022-0252

Barbraud, C., & Delord, K. (2021). Selection against immigrants in wild seabird populations. *Ecology Letters*, *24*(1), 84–93. https://doi.org/10.1111/ele.13624

Beacham, T. D., & Murray, C. B. (1990). Temperature, Egg Size, and Development of Embryos and Alevins of Five Species of Pacific Salmon: A Comparative Analysis. *Transactions of the American Fisheries Society*, *119*(6), 927–945. https://doi.org/10.1577/1548-8659(1990)119<0927:TESADO>2.3.CO;2

Beall, E. (1994). Dispersal patterns and survival of Atlantic salmon (*Salmo salar L.*) juveniles in a nursery stream. *ICES Journal of Marine Science*, *51*(1), 1–9. https://doi.org/10.1006/jmsc.1994.1001

Beechie, T. J., Liermann, M., Beamer, E. M., & Henderson, R. (2005). A Classification of Habitat Types in a Large River and Their Use by Juvenile Salmonids. *Transactions of the American Fisheries Society*, *134*(3), 717–729. https://doi.org/10.1577/T04-062.1

Beverton, R. J. H., & Holt, S. J. (1993). *On the Dynamics of Exploited Fish Populations*. Springer Netherlands. https://doi.org/10.1007/978-94-011-2106-4

Bisson, P. A., Sullivan, K., & Nielsen, J. L. (1988). Channel Hydraulics, Habitat Use, and Body Form of Juvenile Coho Salmon, Steelhead, and Cutthroat Trout in Streams. *Transactions of the American Fisheries Society*, *117*(3), 262–273. https://doi.org/10.1577/1548-8659(1988)117<0262:CHHUAB>2.3.CO;2

Bjornn, T. C., & Reiser, D. W. (n.d.). *Habitat Requirements of Salmonids in Streams*.

Bley, P. W., & Moring, J. R. (1988). *Freshwater and ocean survival of Atlantic salmon and steelhead: A synopsis*. US Fish and Wildlife Service Vol 88 No. 9.

Brunsdon, E. B., Fraser, D. J., Ardren, W. R., & Grant, J. W. A. (2017a). Dispersal and density-dependent growth of Atlantic salmon (*Salmo salar*) juveniles: Clumped versus dispersed stocking. *Canadian Journal of Fisheries and Aquatic Sciences*, *74*(9), 1337–1347. https://doi.org/10.1139/cjfas-2015-0488

Brunsdon, E. B., Fraser, D. J., Ardren, W. R., & Grant, J. W. A. (2017b). Dispersal and density-dependent growth of Atlantic salmon (*Salmo salar*) juveniles: Clumped versus dispersed stocking. *Canadian Journal of Fisheries and Aquatic Sciences*, *74*(9), 1337–1347. https://doi.org/10.1139/cjfas-2015-0488

Cattanéo, F., Lamouroux, N., Breil, P., & Capra, H. (2002). The influence of hydrological and biotic processes on brown trout (*Salmo trutta*) population dynamics. *Canadian Journal of Fisheries and Aquatic Sciences*, *59*(1), 12–22. https://doi.org/10.1139/f01-186

Charnov, E. L. (1976). Optimal foraging, the marginal value theorem. *Theoretical Population Biology*, *9*(2), 129–136. https://doi.org/10.1016/0040-5809(76)90040-X

Close, T. L., & Anderson, C. S. (1992). Dispersal, Density-Dependent Growth, and Survival of Stocked Steelhead Fry in Lake Superior Tributaries. *North American Journal of Fisheries Management*, *12*(4), 728–735. https://doi.org/10.1577/1548-8675(1992)012<0728:DDDGAS>2.3.CO;2

Crisp, D. T. (1993). Population Densities of Juvenile Trout (Salmo trutta) in Five Upland Streams and Their Effects Upon Growth, Survival and Dispersal. *The Journal of Applied Ecology*, *30*(4), 759. https://doi.org/10.2307/2404254

Crozier, W. W., & Kennedy, G. J. A. (1995). Application of a fry (0+;) abundance index, based on semi-quantitative electrofishing, to predict Atlantic salmon smolt runs in the River Bush, Northern Ireland. *Journal of Fish Biology*, *47*(1), 107–114. https://doi.org/10.1111/j.1095-8649.1995.tb01877.x

Dunham, J. B., & Vinyard, G. L. (1997). *Relationships between body mass, population density, and the self-thinning rule in stream-living salmonids*. *54*.

Egglishaw, H. J., & Shackley, P. E. (1980). Survival and growth of salmon, *Salmo salar* (L.), planted in a Scottish stream. *Journal of Fish Biology*, *16*(5), 565–584. https://doi.org/10.1111/j.1095-8649.1980.tb03734.x

Einum, S., & Nislow, K. H. (2005). Local-scale density-dependent survival of mobile organisms in continuous habitats: An experimental test using Atlantic salmon. *Oecologia*, *143*(2), 203–210. https://doi.org/10.1007/s00442-004-1793-y

Einum, S., Nislow, K. H., Mckelvey, S., & Armstrong, J. D. (2008). Nest distribution shaping within-stream variation in Atlantic salmon juvenile abundance and competition over small spatial scales. *Journal of Animal Ecology*, *77*(1), 167–172. https://doi.org/10.1111/j.1365-2656.2007.01326.x

Einum, S., Nislow, K. H., Reynolds, J. D., & Sutherland, W. J. (2008). Predicting population responses to restoration of breeding habitat in Atlantic salmon. *Journal of Applied Ecology*, *45*(3), 930–938. https://doi.org/10.1111/j.1365-2664.2008.01464.x

Einum, S., Robertsen, G., Nislow, K. H., McKelvey, S., & Armstrong, J. D. (2011). The spatial scale of density-dependent growth and implications for dispersal from nests in juvenile Atlantic salmon. *Oecologia*, *165*(4), 959–969. https://doi.org/10.1007/s00442-010-1794-y

Elliott, J. M. (1985). The choice of stock-recruitment model for migratory trout, Salmo trutta, in an English Lake District stream. *Archiv f. Hydrobiologie*, *104*, 145–168.

Elliott, J. M. (1996). The relationship between smolt density and fry density in salmonids. *Journal of Fish Biology*, *48*(5), 1030–1032. https://doi.org/10.1111/j.1095-8649.1996.tb01500.x

Elliott, J. M. (2023). *Quantitative ecology and the brown trout*. Oxford University Press.

Everest, F. H. (1973). *Ecology and Management of Summer Steelhead in the Rogue River*. Oregon State Game Commission.

Everest, F. H., & Chapman, D. W. (1972). Habitat Selection and Spatial Interaction by Juvenile Chinook Salmon and Steelhead Trout in Two Idaho Streams. *Journal of the Fisheries Research Board of Canada*, *29*(1), 91–100. https://doi.org/10.1139/f72-012

Falcy, M. R. (2015). Density-dependent habitat selection of spawning Chinook salmon: Broad-scale evidence and implications. *Journal of Animal Ecology*, *84*(2), 545–553. https://doi.org/10.1111/1365-2656.12297

Faudskar, J. D. (1980). *Ecology of underyearling summer Steelhead trout in intermittent streams tributary to the Rogue*. Masters Thesis, Oregon State University.

Fausch, K. D., Hawkes, C. L., & Parsons, M. G. (1988). *Models That Predict Standing Crop of Stream Fish From Habitat Variables: 1950-85* (No. PNW-GTR-213). US Forest Service. https://www.fs.usda.gov/pnw/pubs/pnw_gtr213.pdf

Finstad, A. G., Sættem, L. M., & Einum, S. (2013). Historical abundance and spatial distributions of spawners determine juvenile habitat accessibility in salmon: Implications for population dynamics and management targets. *Canadian Journal of Fisheries and Aquatic Sciences*, *70*(9), 1339–1345. https://doi.org/10.1139/cjfas-2012-0455

Fleming, I. A. (1996). Reproductive strategies of Atlantic salmon: Ecology and evolution. *Reviews in Fish Biology and Fisheries*, *6*(4), 379–416. https://doi.org/10.1007/BF00164323

Foldvik, A., Finstad, A. G., & Einum, S. (2010). Relating juvenile spatial distribution to breeding patterns in anadromous salmonid populations. *Journal of Animal Ecology*, *79*(2), 501–509. https://doi.org/10.1111/j.1365-2656.2009.01652.x

Fuiman, L. A., & Werner, R. G. (Eds.). (2002). *Fishery science: The unique contributions of early life stages*. Blackwell Science.

Fullerton, A. H., Lindley, S. T., Pess, G. R., Feist, B. E., Steel, E. A., & McElhaney, P. (2011). Human Influence on the Spatial Structure of Threatened Pacific Salmon Metapopulations: Human Influence on Salmon Spatial Structure. *Conservation Biology*, *25*(5), 932–944. https://doi.org/10.1111/j.1523-1739.2011.01718.x

Gallagher, S. P., Ferreira, J., Lang, E., Holloway, W., & Wright, D. W. (2014). Investigation of the relationship between physical habitat and salmonid abundance in two coastal northern California streams. *California Fish and Game*, *100*(4), 683–702.

Gaston, K. J., Blackburn, T. M., Greenwood, J. J. D., Gregory, R. D., Quinn, R. M., & Lawton, J. H. (2000a). Abundance–occupancy relationships. *Journal of Applied Ecology*, *37*(s1), 39–59. https://doi.org/10.1046/j.1365-2664.2000.00485.x

Gaston, K. J., Blackburn, T. M., Greenwood, J. J. D., Gregory, R. D., Quinn, R. M., & Lawton, J. H. (2000b). Abundance–occupancy relationships. *Journal of Applied Ecology*, *37*(s1), 39–59. https://doi.org/10.1046/j.1365-2664.2000.00485.x

Gibson, A. J. F., Bowlby, H. D., & Amiro, P. G. (2008). Are wild populations ideally distributed? Variations in density-dependent habitat use by age class in juvenile Atlantic salmon (Salmo salar). *Canadian Journal of Fisheries and Aquatic Sciences*, *65*(8), 1667–1680. https://doi.org/10.1139/F08-087

Graynoth, E. (1999). Recruitment and distribution of juvenile salmonids in Lake Coleridge, New Zealand. *New Zealand Journal of Marine and Freshwater Research*, *33*(2), 205–219. https://doi.org/10.1080/00288330.1999.9516871

Groot, C., & Margolis, L. (Eds.). (1991). *Pacific salmon life histories*. UBC Press.

Gurney, W. S. C., Bacon, P. J., Tyldesley, G., & Youngson, A. F. (2008). Process-based modelling of decadal trends in growth, survival, and smolting of wild salmon (Salmo salar) parr in a Scottish upland stream. *Canadian Journal of Fisheries and Aquatic Sciences*, *65*(12), 2606–2622. https://doi.org/10.1139/F08-149

Hamann, E. J., & Kennedy, B. P. (2012). Juvenile dispersal affects straying behaviors of adults in a migratory population. *Ecology*, *93*(4), 733–740. https://doi.org/10.1890/11-1009.1

Hankin, D. G., & Reeves, G. H. (1988). Estimating Total Fish Abundance and Total Habitat Area in Small Streams Based on Visual Estimation Methods. *Canadian Journal of Fisheries and Aquatic Sciences*, *45*(5), 834–844. https://doi.org/10.1139/f88-101

Hartman, G. F., & Brown, T. G. (1987). Use of Small, Temporary, Floodplain Tributaries by Juvenile Salmonids in a West Coast Rain-Forest Drainage Basin, Carnation Creek, British Columbia. *Canadian Journal of Fisheries and Aquatic Sciences*, *44*(2), 262–270. https://doi.org/10.1139/f87-035

Hodge, B. W., Wilzbach, M. A., & Duffy, W. G. (2014). Potential Fitness Benefits of the Half-Pounder Life History in Klamath River Steelhead. *Transactions of the American Fisheries Society*, *143*(4), 864–875. https://doi.org/10.1080/00028487.2014.892536

Hume, J. M. B., & Parkinson, E. A. (1987). Effect of Stocking Density on the Survival, Growth, and Dispersal of Steelhead Trout Fry (*Salmo gairdneri*). *Canadian Journal of Fisheries and Aquatic Sciences*, *44*(2), 271–281. https://doi.org/10.1139/f87-036

Hume, J. M. B., & Parkinson, E. A. (1988). Effects of Size at and Time of Release on the Survival and Growth of Steelhead Fry Stocked in Streams. *North American Journal of Fisheries Management*, *8*(1), 50–57. https://doi.org/10.1577/1548-8675(1988)008<0050:EOSAAT>2.3.CO;2

Imre, I., Grant, J. W. A., & Cunjak, R. A. (2005). Density-dependent growth of young-of-the-year Atlantic salmon *Salmo salar* in Catamaran Brook, New Brunswick. *Journal of Animal Ecology*, *74*(3), 508–516. https://doi.org/10.1111/j.1365-2656.2005.00949.x

Isaak, D. J., & Thurow, R. F. (2006). Network-scale spatial and temporal variation in Chinook salmon (*Oncorhynchus tshawytscha*) redd distributions: Patterns inferred from spatially continuous replicate surveys. *Canadian Journal of Fisheries and Aquatic Sciences*, *63*(2), 285–296. https://doi.org/10.1139/f05-214

Isaak, D. J., Thurow, R. F., Rieman, B. E., & Dunham, J. B. (2007). Chinook salmon use of spawning patches: relative roles of habitat quality, size, and connectivity. *Ecological Applications*, *17*(2), 352–364. https://doi.org/10.1890/05-1949

Jenkins, T. M., Diehl, S., Kratz, K. W., & Cooper, S. D. (1999). Effects of population density on individual growth of brown trout in streams. *Ecology*, *80*(3), 941–956. https://doi.org/10.1890/0012-9658(1999)080[0941:EOPDOI]2.0.CO;2

Keeley, E. R. (2001). Demographic responses to food and space competition by juvenile steelhead trout. *Ecology*, 82(5), 1247-1259.

Kwain, W.-H., & McCauley, R. W. (1978). Effects of Age and Overhead Illumination on Temperatures Preferred by Underyearling Rainbow Trout, *Salmo gairdneri* , in a Vertical Temperature Gradient. *Journal of the Fisheries Research Board of Canada*, *35*(11), 1430–1433. https://doi.org/10.1139/f78-225

Lawrence, W. M. (1941). The effect of temperature on the weight of fasting rainbow trout fingerlings. *Transactions of the American Fisheries Society*, *70*(1), 290-296.

Lawson, A. (2006). *Statistical methods in spatial epidemiology* (Second edition). John Wiley & Sons, Ltd. https://doi.org/10.1002/9780470035771

Mangel, M., & Munch, S. B. (2005). A Life-History Perspective on Short- and Long-Term Consequences of Compensatory Growth. *The American Naturalist*, *166*(6), E155–E176. https://doi.org/10.1086/444439

Matte, J. O., Fraser, D. J., & Grant, J. W. A. (2021). Mechanisms of density dependence in juvenile salmonids: Prey depletion, interference competition, or energy expenditure? *Ecosphere*, *12*(6), e03567. https://doi.org/10.1002/ecs2.3567

May, S. A., Shedd, K. R., Rand, P. S., & Westley, P. A. H. (2023). Tidal gradients, fine-scale homing and a potential cryptic ecotype of wild spawning pink salmon (*Oncorhynchus gorbuscha*). *Molecular Ecology*, *32*(21), 5838–5848. https://doi.org/10.1111/mec.17154

McGlauflin, M. T., Schindler, D. E., Seeb, L. W., Smith, C. T., Habicht, C., & Seeb, J. E. (2011). Spawning Habitat and Geography Influence Population Structure and Juvenile Migration Timing of Sockeye Salmon in the Wood River Lakes, Alaska. *Transactions of the American Fisheries Society*, *140*(3), 763–782. https://doi.org/10.1080/00028487.2011.584495

McMillan, J. R., Liermann, M. C., Starr, J., Pess, G. R., & Augerot, X. (2013). Using a Stream Network Census of Fish and Habitat to Assess Models of Juvenile Salmonid Distribution. *Transactions of the American Fisheries Society*, *142*(4), 942–956. https://doi.org/10.1080/00028487.2013.790846

Milner, N. J., Elliott, J. M., Armstrong, J. D., Gardiner, R., Welton, J. S., & Ladle, M. (2003). The natural control of salmon and trout populations in streams. *Fisheries Research*, *62*(2), 111–125. https://doi.org/10.1016/S0165-7836(02)00157-1

Milner, N. J., Gee, A. S., & Hemsworth, R. J. (1979). Recruitment and turnover of populations of brown trout, *Salmo trutta* , in the upper River Wye, Wales. *Journal of Fish Biology*, *15*(2), 211–222. https://doi.org/10.1111/j.1095-8649.1979.tb03584.x

Mobley, K. B., Granroth-Wilding, H., Ellmen, M., Vähä, J.-P., Aykanat, T., Johnston, S. E., Orell, P., Erkinaro, J., & Primmer, C. R. (2019). Home ground advantage: Local Atlantic salmon have higher reproductive fitness than dispersers in the wild. *Science Advances*, *5*(2), eaav1112. https://doi.org/10.1126/sciadv.aav1112

Moussalli, E., & Hilborn, R. (1986). Optimal Stock Size and Harvest Rate in Multistage Life History Models. *Canadian Journal of Fisheries and Aquatic Sciences*, *43*(1), 135–141. https://doi.org/10.1139/f86-014

Neville, H. M., Isaak, D. J., Dunham, J. B., Thurow, R. F., & Rieman, B. E. (2006). Fine-scale natal homing and localized movement as shaped by sex and spawning habitat in Chinook salmon: Insights from spatial autocorrelation analysis of individual genotypes. *Molecular Ecology*, *15*(14), 4589–4602. https://doi.org/10.1111/j.1365-294X.2006.03082.x

Noble, S. M. (1991). *Impacts of Earlier Emerging Steelhead Fry of Hatchery Origin on the Social Structure, Distribution, and Growth of Wild Steelhead Fry*. Masters Thesis, Oregon State University

Peterson, D. A., Hilborn, R., & Hauser, L. (2014). Local adaptation limits lifetime reproductive success of dispersers in a wild salmon metapopulation. *Nature Communications*, *5*(1), 3696. https://doi.org/10.1038/ncomms4696

Quinn, T. P. (2018). *The behavior and ecology of Pacific salmon and trout* (Second edition). University of Washington Press ; In association with American Fisheries Society.

Quinn, T. P., Stewart, I. J., & Boatright, C. P. (2006). Experimental evidence of homing to site of incubation by mature sockeye salmon, Oncorhynchus nerka. *Animal Behaviour*, *72*(4), 941–949. https://doi.org/10.1016/j.anbehav.2006.03.003

R Core Team. (2025). *R: A language and environment for statistical computing*. R Foundation for Statistical Computing. https://www.R-project.org/

Ricker, W. E. (1954). Stock and Recruitment. *Journal of the Fisheries Research Board of Canada*, *11*(5), 559–623. https://doi.org/10.1139/f54-039

Ricker, W. E. (1963). Big Effects from Small Causes: Two Examples from Fish Population Dynamics. *Journal of the Fisheries Research Board of Canada*, *20*(2), 257–264. https://doi.org/10.1139/f63-022

Riedel, J., Sarrantonio, S., Seixas, G., & Clement, C. (2025). *Skagit River Geomorphology*. Seattle City Light.

Roff, D. A. (1991). Life History Consequences of Bioenergetic and Biomechanical Constraints on Migration. *American Zoologist*, *31*(1), 205–216. https://doi.org/10.1093/icb/31.1.205

Scheuerell, M. D., Ruff, C. P., Anderson, J. H., & Beamer, E. M. (2021). An integrated population model for estimating the relative effects of natural and anthropogenic factors on a threatened population of steelhead trout. *Journal of Applied Ecology*, *58*(1), 114–124. https://doi.org/10.1111/1365-2664.13789

Schtickzelle, N., & Quinn, T. P. (2007). A metapopulation perspective for salmon and other anadromous fish. *Fish and Fisheries*, *8*(4), 297–314. https://doi.org/10.1111/j.1467-2979.2007.00256.x

Sogard, S. M., Williams, T. H., & Fish, H. (2009). Seasonal Patterns of Abundance, Growth, and Site Fidelity of Juvenile Steelhead in a Small Coastal California Stream. *Transactions of the American Fisheries Society*, *138*(3), 549–563. https://doi.org/10.1577/T08-172.1

Thurow, R. F. (1994). *Underwater methods for study of salmonids in the Intermountain West*. (General Technical Report INT-GTR-307). U.S. Department of Agriculture, Forest Service, Intermountain Research Station.

Thurow, R. F., Copeland, T., & Oldemeyer, B. N. (2020). Wild salmon and the shifting baseline syndrome: Application of archival and contemporary redd counts to estimate historical Chinook salmon (*Oncorhynchus tshawytscha*) production potential in the central Idaho wilderness. *Canadian Journal of Fisheries and Aquatic Sciences*, *77*(4), 651–665. https://doi.org/10.1139/cjfas-2019-0111

Vincenzi, S., Satterthwaite, W. H., & Mangel, M. (2012). Spatial and temporal scale of density-dependent body growth and its implications for recruitment, population dynamics and management of stream-dwelling salmonid populations. *Reviews in Fish Biology and Fisheries*, *22*(3), 813–825. https://doi.org/10.1007/s11160-011-9247-1

Walters, A. W., Copeland, T., & Venditti, D. A. (2013). The density dilemma: Limitations on juvenile production in threatened salmon populations. *Ecology of Freshwater Fish*, *22*(4), 508–519. https://doi.org/10.1111/eff.12046

Ward, B. R., & Slaney, P. A. (1993). Egg to Smolt Survival Fry to Smolt Density Dependence of Keogh River Steelhead Trout. *In R.J. Gibson and R.E. Cutting [Ed.] Can. Spec. Publ. Fish. Aquat. Sci*, *118*.

Ward, D. M., Nislow, K. H., Armstrong, J. D., Einum, S., & Folt, C. L. (2007). Is the shape of the density–growth relationship for stream salmonids evidence for exploitative rather than interference competition? *Journal of Animal Ecology*, *76*(1), 135–138. https://doi.org/10.1111/j.1365-2656.2006.01169.x

Wentworth, R. S., & Labar, G. W. (1984). First-Year Survival and Growth of Steelhead Stocked as Fry in Lewis Creek, Vermont. *North American Journal of Fisheries Management*, *4*(1), 103–110. https://doi.org/10.1577/1548-8659(1984)4<103:FSAGOS>2.0.CO;2

Williams, R. W., & Phinney, L. A. (1975). *A Catalog of Washington streams and salmon utilization. Washington Dept. Of*. Washington Department of Fisheries. https://docs.streamnetlibrary.org/WashingtonStreamCatalog/WRIAs.pdf

Wright, J., Solbu, E. B., & Engen, S. (2020). Contrasting patterns of density-dependent selection at different life stages can create more than one fast–slow axis of life-history variation. *Ecology and Evolution*, *10*(6), 3068–3078. https://doi.org/10.1002/ece3.6122

Appendix 1: Model Structure and Equations

The models and formulations here follow forms described in Gelman et. al. (2013).

Notation and Symbols

Symbols and definitions for variables used in all models.

y_i = Observed fry location (distance from origin) for individual i
N_f = Total number of fry observations
z_i = Latent cluster assignment for fry i
K = Total number of clusters (redds)
μ_k = Mean of the distribution for cluster k
μ_1 = Mean of the first cluster (used as a reference)
d_k = Offset from reference cluster to cluster k
$\mathbf{p}$ = Vector of cluster probabilities $(p_1, \dots, p_K)$
$\boldsymbol{\alpha}$ = Dirichlet concentration parameters
σ^2 = Variance of normal/lognormal distribution
τ = Precision, where $\tau = \frac{1}{\sigma^2}$
θ = Gamma shape parameter
μ_k (Gamma) = Mean of gamma distribution for cluster k
β_k = $\frac{\theta}{\mu_k}$ (Rate parameter of gamma)
$\Gamma(\cdot)$ = Gamma function

Models for Single Isolated Redds

Models for single redds were fit using the probability density functions likelihood for estimating the mean and variance of statistical distributions used to describe the patterns of fry distribution near redds.

Normal distribution:

$$\text{PDF:} \quad L(\mu, \sigma) = \prod_{j=1}^{N} \frac{1}{\sqrt{2\pi\sigma^2}} \exp\left(-\frac{\left(y_j - \mu_{s_j}\right)^2}{2\sigma^2} \right)$$

Lognormal distribution:

$$\text{PDF:} \quad L(\mu,\sigma) = \prod_{j=1}^{N} \frac{1}{y_j\sqrt{2\pi\sigma^2}} \exp\left(-\frac{\left(\log y_j - \mu_{s_j}\right)^2}{2\sigma^2}\right)$$

Gamma distribution:

We parameterized the gamma distribution using shape (θ) and mean (μ), such that the rate was defined as θ/μ. This ensures the expected value is μ, while the variance is μ^2/θ.This allowed for conversion of estimated shape and rate values into meaningful terms, namely the expected mean and variance of dispersal kernels.

$$\text{PDF:} \quad L(\mu,\theta) = \prod_{j=1}^{N} \frac{\left(\frac{\theta}{\mu_{s_j}}\right)^{\theta}}{\Gamma(\theta)} y_j^{\theta-1} \exp\left(-\frac{\theta}{\mu_{s_j}} y_j\right)$$

Models for Clustered Redds

Model 1: Categorical assignment of fry to observed redds

In this model, we assume that the relative positions of redds within a site are known and we estimate a common location offset for the entire group. Each fry is assumed to be drawn from a distribution centered at a redd location, with assignment drawn from a categorical distribution weighted by relative redd contribution.

Model Structure: shared across all variants

$$\begin{aligned}
\mu_1 &\sim \text{Normal} + (0,10^4) \quad \text{(location of reference redd)} \\
\mu_k &= \mu_1 + d_k \quad \text{for } k = 2,\ldots,K \quad \text{(offset redd locations)} \\
\mathbf{p} &\sim \text{Dirichlet}(\boldsymbol{\alpha}) \\
z_i &\sim \text{Categorical}(\mathbf{p}) \text{ (categorical assignment of fry)} \\
\mu_i &= \mu_{z_i} \text{ (mean of each dispersal kernel)}
\end{aligned}$$

Each iteration of Model 1 differs in the assumed distribution of fry distances as shown below.

1. Normal Distribution

$$\text{Prior:} \quad \tau \sim \text{Gamma}(1,1)$$

$$\text{Conditional PDF:} \quad f(y_i \mid z_i = k, \mu_k, \sigma^2) = \frac{1}{\sqrt{2\pi\sigma^2}} \exp\left(-\frac{(y_i - \mu_k)^2}{2\sigma^2}\right)$$

$$\text{Marginal likelihood:} \quad f(y_i \mid \boldsymbol{\mu}, \sigma^2, \mathbf{p}) = \sum_{k=1}^{K} p_k \cdot \frac{1}{\sqrt{2\pi\sigma^2}} \exp\left(-\frac{(y_i - \mu_k)^2}{2\sigma^2}\right)$$

2. Lognormal Distribution

$$\text{Prior:} \quad \tau \sim \text{Gamma}(1,1)$$

$$\text{Conditional PDF:} \quad f(y_i \mid z_i = k, \mu_k, \sigma^2) = \frac{1}{y_i\sqrt{2\pi\sigma^2}} \exp\left(-\frac{(\log y_i - \mu_k)^2}{2\sigma^2}\right)$$

$$\text{Marginal likelihood:} \quad f(y_i \mid \boldsymbol{\mu}, \sigma^2, \mathbf{p}) = \sum_{k=1}^{K} p_k \cdot \frac{1}{y_i\sqrt{2\pi\sigma^2}} \exp\left(-\frac{(\log y_i - \mu_k)^2}{2\sigma^2}\right)$$

3. Gamma Distribution

We parameterize the gamma distribution using shape θ and mean μ_k, with rate $\beta_k = \theta/\mu_k$.

$$\text{Prior:} \quad \theta \sim \text{Gamma}(1,1)$$

$$\text{Conditional PDF:} \quad f(y_i \mid z_i = k, \mu_k, \theta) = \frac{\left(\frac{\theta}{\mu_k}\right)^{\theta}}{\Gamma(\theta)} y_i^{\theta-1} \exp\left(-\frac{\theta}{\mu_k} y_i\right)$$

$$\text{Marginal likelihood:} \quad f(\, y_i \mid \boldsymbol{\mu}, \theta, \mathbf{p}\,) = \sum_{k=1}^{K} p_k \cdot \frac{\left(\frac{\theta}{\mu_k}\right)^{\theta}}{\Gamma(\theta)} y_i^{\theta-1} \exp(-\theta/\mu\_k \;\; y\_i\,)$$

Model 2

Probabilistic assignment of fry to redd locations.

Observed fry distances $\{y_i\}_{i=1}^{N_f}$ were modeled using a finite mixture model with K redds. Each observation is assumed to be drawn from a redd specific dispersal kernel (parametric distribution), with cluster membership assigned probabilistically via a categorical distribution.

Model Structure: shared across all models

$$\begin{aligned} z_i &\sim \text{Categorical}(p_1, \ldots, p_K) \quad \text{(probabilistic assignment)} \\ \mu_k &= \mu_1 + d_k \quad \text{for } k = 2, \ldots, K \quad \text{(offset redd locations)} \\ \mathbf{p} &\sim \text{Dirichlet}(\boldsymbol{\alpha}) \quad \text{(redd assignment probabilities)} \end{aligned}$$

The cluster-specific observation model varies by distribution:

1. Normal Distribution

$$\text{Prior:} \quad \tau \sim \text{Gamma}(1, 1)$$

$$\text{Conditional PDF:} \quad f(y_i \mid z_i = k, \mu_k, \sigma^2) = \frac{1}{\sqrt{2\pi\sigma^2}} \exp\left(-\frac{(y_i - \mu_k)^2}{2\sigma^2}\right)$$

$$\text{Marginal likelihood:} \quad f(y_i \mid \boldsymbol{\mu}, \sigma^2, \mathbf{p}) = \sum_{k=1}^{K} p_k \cdot \frac{1}{\sqrt{2\pi\sigma^2}} \exp\left(-\frac{(y_i - \mu_k)^2}{2\sigma^2}\right)$$

Lognormal Distribution

$$\text{Prior:} \quad \tau \sim \text{Gamma}(1, 1)$$

$$\text{Conditional PDF:} \quad f(y_i \mid z_i = k, \mu_k, \sigma^2) = \frac{1}{y_i\sqrt{2\pi\sigma^2}} \exp\left(-\frac{(\log y_i - \mu_k)^2}{2\sigma^2}\right)$$

$$\text{Marginal likelihood:} \quad f(y_i \mid \boldsymbol{\mu}, \sigma^2, \mathbf{p}) = \sum_{k=1}^{K} p_k \cdot \frac{1}{y_i\sqrt{2\pi\sigma^2}} \exp\left(-\frac{(\log y_i - \mu_k)^2}{2\sigma^2}\right)$$

3. Gamma distribution

We parameterize the gamma distribution using shape θ and mean μ_k, with rate $\beta_k = \theta/\mu_k$.

$$\text{Prior:} \quad \tau \sim \text{Gamma}(1,1)$$

$$\text{Conditional PDF:} \quad f(y_i \mid z_i = k, \mu_k, \theta) = \frac{\left(\frac{\theta}{\mu_k}\right)^{\theta}}{\Gamma(\theta)} y_i^{\theta-1} \exp\left(-\frac{\theta}{\mu_k} y_i\right)$$

$$\text{Marginal likelihood:} \quad f(y_i \mid \boldsymbol{\mu}, \theta, \mathbf{p}) = \sum_{k=1}^{K} p_k \cdot \frac{\left(\frac{\theta}{\mu_k}\right)^{\theta}}{\Gamma(\theta)} y_i^{\theta-1} \exp\left(-\frac{\theta}{\mu_k} y_i\right)$$

Model 3

Assignment of fry to latent redd locations

We model observed fry distances $\{y_i\}_{i=1}^{N_f}$ as arising from a finite mixture model with K latent redds. In this model, the locations of the redds are not known a priori and are inferred from the data. Each fry is assumed to be drawn from a specific redd distribution, with natal redd assigned probabilistically.

Model Structure : shared across all variants

$$\begin{aligned} z_i &\sim \text{Categorical}(p_1, \ldots, p_K) \quad \text{(redd assignment)} \\ \mu_k &\sim \text{Prior (see below)} \quad \text{(unknown redd locations)} \\ \mathbf{p} &\sim \text{Dirichlet}(\boldsymbol{\alpha}) \quad \text{(redd assignment probability)} \end{aligned}$$

1. Normal Distribution

$$\text{Priors:} \quad \begin{aligned} \mu_k &\sim \text{Normal}(0, 10^4) \\ \tau &\sim \text{Gamma}(1,1) \end{aligned}$$

Conditional PDF: $f(y_i \mid z_i = k, \mu_k, \sigma^2) = \frac{1}{\sqrt{2\pi\sigma^2}} \exp\left(-\frac{(y_i - \mu_k)^2}{2\sigma^2}\right)$

Marginal likelihood: $f(y_i \mid \boldsymbol{\mu}, \sigma^2, \mathbf{p}) = \sum_{k=1}^{K} p_k \cdot \frac{1}{\sqrt{2\pi\sigma^2}} \exp\left(-\frac{(y_i - \mu_k)^2}{2\sigma^2}\right)$

2. Lognormal Distribution

Priors: $\begin{aligned} \mu_k &\sim \text{Normal}(0, 10^4) \\ \tau &\sim \text{Gamma}(1,1) \end{aligned}$

Conditional PDf: $f(y_i \mid z_i = k, \mu_k, \sigma^2) = \frac{1}{y_i\sqrt{2\pi\sigma^2}} \exp\left(-\frac{(\log y_i - \mu_k)^2}{2\sigma^2}\right)$

Marginal likelihood: $f(y_i \mid \boldsymbol{\mu}, \sigma^2, \mathbf{p}) = \sum_{k=1}^{K} p_k \cdot \frac{1}{y_i\sqrt{2\pi\sigma^2}} \exp\left(-\frac{(\log y_i - \mu_k)^2}{2\sigma^2}\right)$

3. Gamma Distribution

We parameterize the gamma distribution using shape θ and mean μ_k, with rate $\beta_k = \theta/\mu_k$.

Priors: $\begin{aligned} \mu_k &\sim \text{Gamma}(2,0.001) \\ \theta &\sim \text{Gamma}(0.01,0.01) \end{aligned}$

Conditional PDF: $f(y_i \mid z_i = k, \mu_k, \theta) = \frac{\left(\frac{\theta}{\mu_k}\right)^{\theta}}{\Gamma(\theta)} y_i^{\theta-1} \exp\left(-\frac{\theta}{\mu_k} y_i\right)$

Marginal likelihood: $f(y_i \mid \boldsymbol{\mu}, \theta, \mathbf{p}) = \sum_{k=1}^{K} p_k \cdot \frac{\left(\frac{\theta}{\mu_k}\right)^{\theta}}{\Gamma(\theta)} y_i^{\theta-1} \exp\left(-\frac{\theta}{\mu_k} y_i\right)$